

# A Framework for Supervised Heterogeneous Transfer Learning using Dynamic Distribution Adaptation and Manifold Regularization

Md Geaur Rahman\*, Md Zahidul Islam\*\*

*School of Computing, Mathematics and Engineering, Charles Sturt University, Australia*

---

## Abstract

Transfer learning aims to learn classifiers for a target domain by transferring knowledge from a source domain. However, due to two main issues: feature discrepancy and distribution divergence, transfer learning can be a very difficult problem in practice. In this paper, we present a framework called TLF that builds a classifier for the target domain having only few labeled training records by transferring knowledge from the source domain having many labeled records. While existing methods often focus on one issue and leave the other one for the further work, TLF is capable of handling both issues simultaneously. In TLF, we alleviate feature discrepancy by identifying shared label distributions that act as the pivots to bridge the domains. We handle distribution divergence by simultaneously optimizing the structural risk functional, joint distributions between domains, and the manifold consistency underlying marginal distributions. Moreover, for the manifold consistency we exploit its intrinsic properties by identifying  $k$  nearest neighbors of a record, where the value of  $k$  is determined automatically in TLF. Furthermore, since negative transfer is not desired, we consider only the source records that are belonging to the source pivots during the knowledge transfer. We evaluate TLF on seven publicly available natural datasets and compare the performance of TLF against the performance of eleven state-of-the-art techniques. We also evaluate the effectiveness of TLF in some challenging situations. Our experimental results, including statistical sign test and Nemenyi test analyses, indicate a clear superiority of the proposed framework over the state-of-the-art techniques.

**Keywords:** Transfer learning, heterogeneous domain adaptation, manifold regularization, random forest, dynamic distribution adaptation

---



---

\*Corresponding author. Tel: +61 4 8010 0601, <http://gea.bau.edu.bd>

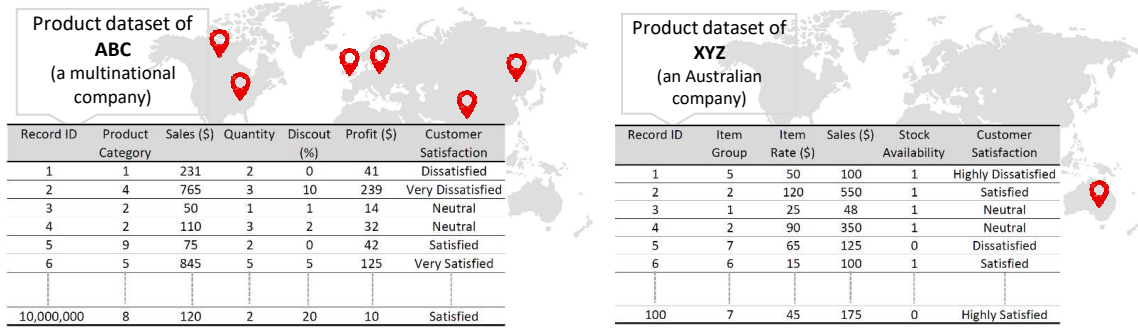
\*\*URL: <http://csusap.csu.edu.au/~zislam/> (Md Zahidul Islam)

Email addresses: [grahman@csu.edu.au](mailto:grahman@csu.edu.au) (Md Geaur Rahman), [zislam@csu.edu.au](mailto:zislam@csu.edu.au) (Md Zahidul Islam)

## 1. Introduction

Nowadays, Transfer Learning (TL) has made breakthroughs in solving real-world problems, including activity recognition, sentiment classification, document analysis and indoor localization [1, 2]. Traditional Machine Learning (ML) methods cannot handle these problems due to various reasons, including insufficient data for building a model and distribution mismatch between training and test datasets [3, 4].

TL algorithms build a model for a domain (often referred to as the target domain), which has insufficient data, by transferring knowledge from single or multiple auxiliary domains (referred to as source domains) [1, 2]. However, commonly used TL methods assume that the source domain dataset (SDD) and target domain dataset (TDD) have the same set of attributes [3, 5]. In addition, traditional supervised TL methods assume that the datasets have the same set of labels [3, 4, 6]. The methods may not perform well if the datasets have different set of attributes and labels [2]. The domains of such datasets often known as heterogeneous domains [2].



**Product dataset of ABC**  
(a multinational company)

Record ID	Product Category	Sales (\$)	Quantity	Discount (%)	Profit (\$)	Customer Satisfaction
1	1	231	2	0	41	Dissatisfied
2	4	765	3	10	239	Very Dissatisfied
3	2	50	1	1	14	Neutral
4	2	110	3	2	32	Neutral
5	9	75	2	0	42	Satisfied
6	5	845	5	5	125	Very Satisfied
10,000,000	8	120	2	20	10	Satisfied

**Product dataset of XYZ**  
(an Australian company)

Record ID	Item Group	Item Rate (\$)	Sales (\$)	Stock Availability	Customer Satisfaction
1	5	50	100	1	Highly Dissatisfied
2	2	120	550	1	Satisfied
3	1	25	48	1	Neutral
4	2	90	350	1	Neutral
5	7	65	125	0	Dissatisfied
6	6	15	100	1	Satisfied
100	7	45	175	0	Highly Satisfied

(a) Source domain: A toy dataset (Product) of a hypothetical multinational company “ABC”

(b) Target domain: A toy dataset (Product) of a hypothetical Australian company “XYZ”

Figure 1: Sample source and target domains using toy datasets.

A hypothetical heterogeneous setting is illustrated in Fig. 1, where Fig. 1a and Fig. 1b show two toy datasets related to products, sales and customer feedback information of a renowned multinational electronics company “ABC” and a newly established Australian superstore “XYZ”, respectively. The datasets are heterogeneous in terms of attributes and labels. The “XYZ” company aims to evaluate the products based on the customer feedback. Since the dataset of “XYZ” company contains only few labeled records, it may not be possible to build a good model by applying an ML algorithm on the dataset. Besides, a good model for the “XYZ” company can be built by transferring records in a compatible way from the dataset of “ABC” company which has many records. However, traditional

TL methods, such as ARTL [3] and MEDA [4] are not capable of transferring knowledge from source to target domain since the datasets have different sets of features and labels.

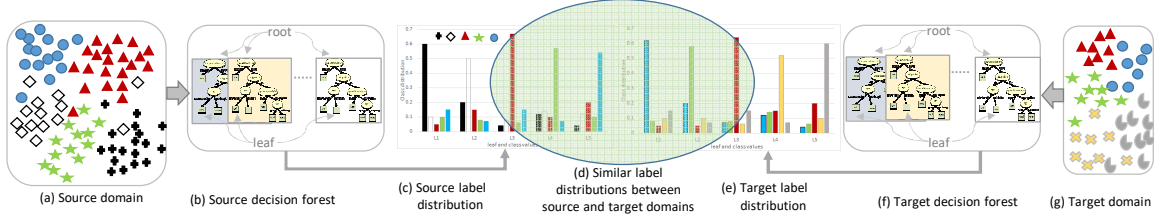


Figure 2: Basic concept of bridging between source and target domains.

For dealing with such settings, a number of heterogeneous transfer learning (HTL) methods have been proposed, and have recently received significant attention in the literature [2, 7]. An existing HTL method called SHDA [2] which deals with such setting by transferring records of SDD to TDD. SHDA projects source records for TDD by identifying similar label distributions that act as the bridge between SDD and TDD. The concept of bridging the domains is illustrated in Fig 2. Using the SDD (Fig. 2a), SHDA builds a decision forest (in short, forest) which consists of a set of decision trees (in short, trees) as shown in Fig. 2b. A tree has a set of rules, where a rule is used to create a leaf (see Fig. 3) containing records that satisfy the conditions of the rule. Using the records of a leaf, SHDA calculates label distributions of the leaf. The hypothetical label distributions of all leaves for the source domain are shown in Fig. 2c. Similarly, for the TDD (Fig. 2g), SHDA builds a forest (Fig. 2f) and then calculates the label distributions of all leaves (Fig. 2e). After that SHDA finds similar label distributions (see Fig. 2d) between the domains. The similar label distributions act as the pivots to bridge the domains and help achieving accurate transfer of data.

For both source and target forests, SHDA then calculates attribute contributions of the leaves that are associated with the pivots (discussed in Section 3). The contribution of an attribute  $A_j$  is calculated as  $(\frac{1}{2})^l$ , where  $l$  is the level of the node where  $A_j$  is contributed. As an example, for Leaf 3 of the sample tree (see Fig. 3) the contribution of attributes “Item Group” and “Sales” are 0.625 ( $=0.500+0.125$ ) and 0.250 respectively. The attribute contributions are then used in Eq. (1) to project the records of SDD into TDD. Combining the projected records with the TDD, SHDA builds the final model as the target model which is then used to classify the test data (discussed in Section 5.2.1).

In HTL, a good method should address two challenging issues [7]: distribution divergence and feature discrepancy. However, existing methods often focus on one issue and leave the other one for the further work. For example, ARTL [3] and MEDA [4] focus on minimizing distribution divergence

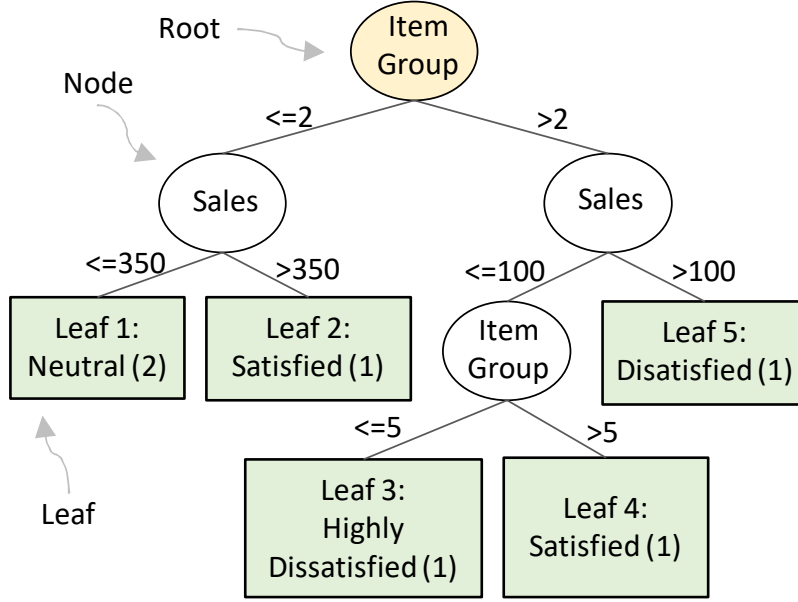


Figure 3: A sample decision tree.

while SHDA [2] attends to learning shared label distributions.

ARTL [3] and MEDA [4] have minimized the conditional distribution divergence by using maximum mean discrepancy (MMD) [8] and marginal distribution divergence by exploiting intrinsic properties of manifold consistency [9]. However, to identify the nearest neighbors of a record during manifold regularization, the methods use a user-defined parameter  $k$  which may fail to exploit the properties accurately (explained later in Section 4.1 and Fig. 5) resulting in a low classification accuracy. Moreover, the methods are unable to handle the feature discrepancy.

The feature discrepancy is handled in SHDA [2] by identifying pivots (discussed earlier) between SDD and TDD, the distribution divergence, however, is not addressed. Moreover, it provides higher weights to parent nodes than their children while calculating attribute contributions. For a leaf, the importance of a test attribute in classifying the records belonging to the leaf does not necessarily depend on the position/level of the attribute in the rule. It also transfers all records from SDD to TDD and may result in negative transfer [7].

The existing methods therefore have room for further improvement. In this paper, we present a novel transfer learning framework called TLF that builds a classifier for TDD by transferring knowledge from SDD. TLF is capable of handling the two issues. The main contributions of TLF are summarized as follows.

- We eliminate the feature discrepancy by identifying pivots between SDD and TDD by following the SHDA’s approach. However, we calculate attribute contributions using the leaf’s centroids (attribute wise mean plus standard deviation) instead of considering the node’s level in the tree path from the root to the leaf used in SHDA (discussed in Section 4.1).
- We minimize distribution divergence by using MMD and manifold simultaneously where the intrinsic property of the manifold consistency is exploited automatically (discussed in Section 4.1).
- We minimize negative transfer, during the projection, by considering only the source records that are belonging to the source pivots (discussed in Section 4.1).

We evaluate TLF on seven publicly available real datasets by comparing its performance with the performance of eleven high quality existing techniques including two baseline algorithms. Our experimental results and statistical analyses indicate that TLF performs significantly better than the existing methods.

The rest of the paper is organized as follows. Section 2 presents problem formulation and assumptions, and Section 3 presents a background study on transfer learning. Our proposed transfer learning framework is presented in Section 4. Section 5 presents experimental results, Section 6 presents the effectiveness of TLF in some challenging situations, and Section 7 gives concluding remarks.

## 2. Problem Formulation

In this section, we define the problem setting, assumptions and goal for supervised heterogeneous transfer learning. The notations that we use frequently in this paper, are presented in Table 1.

**Definition 1.** *Domain [7, 3]: A domain  $D$  is formed by a feature space  $X$  having  $d$  number of attributes and a marginal probability distribution  $P(x)$ , i.e.,  $D = X, P(x)$ , where  $x \in X$ .*

**Definition 2.** *Task [7, 3]: For a domain  $D$ , a task  $T$  is formed by a set of labels  $Y$  and a classification function  $f(x)$ , i.e.,  $T = \{Y, f(x)\}$ , where  $y \in Y$ , and  $f(x) = Q(y|x)$  can be considered as the conditional probability distribution.*

Let  $D_s$  and  $D_t$  be the source domain and target domain, respectively. If the domains have different feature spaces or marginal distributions, i.e.,  $X_s \neq X_t \vee P_s(x_s) \neq P_t(x_t)$  then the domains can

Table 1: Notations and their meanings

Notation	Meaning	Notation	Meaning
$D_s$	Source domain	$D_t$	Target domain
$n_s$	Size of $D_s$	$n_t$	Size of $D_t$
$d_s$	Attributes of $D_s$	$d_t$	Attributes of $D_t$
$X_s$	Records of $D_s$	$X_t$	Records of $D_t$
$Y_s$	Labels of $D_s$	$Y_t$	Labels of $D_t$
$C$	# shared labels	$\mathbf{K}$	Kernel matrix
$\sigma$	Ridge regularization	$\mu$	MMD adaptive factor
$\lambda$	MMD regularization	$\mathbf{M}$	MMD matrix
$\gamma$	Manifold regularization	$\mathbf{L}$	Graph Laplacian matrix

be considered as different i.e.,  $D_s \neq D_t$ . Also, let  $T_s$  and  $T_t$  be the source task and target task, respectively. If the tasks have different labels or conditional distributions, i.e.,  $Y_s \neq Y_t \vee Q_s(y_s|x_s) \neq Q_t(y_t|x_t)$  then the tasks can be considered as different i.e.,  $T_s \neq T_t$ .

**Definition 3.** *Supervised Heterogeneous Transfer Learning (SHTL): Given a source domain having labels i.e.  $D_s = \{(x_{s_1}, y_{s_1}), \dots, (x_{s_{n_s}}, y_{s_{n_s}})\}$  and a target domain having labels i.e.  $D_t = \{(x_{t_1}, y_{t_1}), \dots, (x_{t_{n_t}}, y_{t_{n_t}})\}$ , the goal of SHTL is to build classifier  $f$  on  $D_t$  by learning a mapping  $P : D_s \mapsto D_t$ , under the assumptions  $n_s \gg n_t$ ,  $X_s \cap X_t = \emptyset$ ,  $d_s \cap d_t = d$ ,  $Y_s \cap Y_t = C$ ,  $P_s(x_s) \neq P_t(x_t)$ , and  $Q_s(y_s|x_s) \neq Q_t(y_t|x_t)$ .*

### 3. Related Work

A number of methods have been proposed for heterogeneous transfer learning (HTL) [2, 10, 11]. HTL methods can broadly be classified into 3 categories: *Unsupervised HTL*, *Semi-supervised HTL* and *Supervised HTL* as shown in Table 2. Our proposed framework, TLF falls under *Supervised HTL* category.

Table 2: Heterogeneous transfer learning (HTL) categories.

Category	$Y_s$	$Y_t$	Examples
Unsupervised HTL	No	No	STC [12]
Semi-supervised HTL	Yes	No	ARTL [3], MEDA [4], DASVM [5]
Supervised HTL	Yes	Yes	SHDA [2], TLF [ours]

*Unsupervised HTL* methods deal with the setting where both source and target domains have insufficient or no label records, and are generally applied to tasks that are special and unique [1]. An example of unsupervised HTL method is called STC [12] that performs clustering on target domain,

$D_t$  having small unlabeled records, by utilizing the knowledge obtained from target domain,  $D_s$  having sufficient unlabeled records. STC first transforms both  $D_s$  and  $D_t$  into a common feature space and then uses  $D_s$  to cluster  $D_t$ . However, the methods are found to be difficult to apply to real-world tasks [1].

*Semi-supervised HTL* methods consider the scenario where  $D_s$  has labeled records but  $D_t$  has no label data [13, 4]. The methods initially build a model from  $D_s$  and then apply the model on  $D_t$  to obtain pseudo-labels for the records of  $D_t$ . After that the methods iteratively minimize distribution differences between  $D_s$  and  $D_t$ , and update the pseudo-labels until convergence criteria are met.

An existing method called DASVM [5] initially builds a classifier by applying the support vector machine (SVM) [14] on  $D_s$ . At the first iteration, the records of  $D_s$  are considered as the training set. The classifier is then used to estimate the labels of the records of  $D_t$ . The training set is then iteratively updated by adding  $m$  records, that are classified with high confidence, from  $D_t$  and removing  $m$  records, that have less influence on the classifier, of  $D_s$ . In each iteration, the classifier is also retrained based on the current training set. Since DASVM ultimately builds the final classifier by considering only the records of  $D_t$ , a good classifier may not be built if  $D_t$  contains insufficient records. Moreover, only the structural risk functional (SRF) is minimized in DASVM.

In addition to SRF, ARTL [3] and MEDA [4] minimize the difference between joint distributions of  $D_s$  and  $D_t$  by using maximum mean discrepancy (MMD) [8], and maximize manifold consistency [9] by considering the domains marginal distributions. However, a user requires to provide a value for  $k$ , to exploit the intrinsic property of the manifold consistency, which can be a difficult task of the user in real-world applications. Moreover, in both  $D_s$  and  $D_t$ , the methods require same set of features and expect same set of labels.

*Supervised HTL* methods deal with the setting where both  $D_s$  and  $D_t$  have labeled data and  $n_s \gg n_t$ . Since our proposed framework, TLF belongs to this category, we discuss a recent existing method called SHDA [2] in detail as follows.

SHDA first builds a forest (say 100 trees, a sample tree is shown in Fig. 3) by applying the Random Forest (RF) [15] on  $D_s$  and obtains a set of rules  $R_s$  that produces  $L_s$  leaves. For every rule from the root to a leaf node, it calculates the contribution of each attribute of  $D_s$ . The contribution of an attribute  $d_{s_j} \in d_s$  is calculated as  $W_{s_j} = \sum_{i=1}^v (\frac{1}{2})^{v(i)}$  where  $v$  is a list contains the level numbers at which the attribute  $d_{s_j}$  is considered as the candidate split. Thus for all rules, it produces a contribution matrix  $W_s^{[L_s \times d_s]}$ . After that, for each leaf SHDA calculates the distributions of labels. If the size of the class

attribute of  $D_s$  is  $C_s$  then SHDA produces a label distribution matrix,  $Q_s^{[L_s \times C_s]}$ .

SHDA then refines  $Q_s$  by removing the duplicate rows of the label distribution. For every duplicate row, the corresponding rows of the attributes contribution matrix  $W_s$  are averaged. Similar to  $D_s$ , SHDA produces the attributes contribution matrix  $W_t^{[L_t \times d_t]}$  and label distribution matrix,  $Q_t^{[L_t \times C_t]}$  by building a forest from  $D_t$ , where  $R_t$  is number of rules and  $C_t$  is the size of the class attribute of  $D_t$ . The label distribution  $L_t$  is also refined by removing the duplicate rows, and then the corresponding rows of the attributes contribution matrix  $W_t$  are also averaged.

Using  $Q_s$  and  $Q_t$ , SHDA identifies the identical or similar label distributions across  $D_s$  and  $D_t$ . Let  $N_p$  be the number of identical or similar label distributions across the source and target domains. These  $N_p$  rows of  $Q_s$  and  $Q_t$  are called the pivots that act as the bridge between  $D_s$  and  $D_t$ . The concept of bridging  $D_s$  and  $D_t$  is illustrated in Fig. 2.

Since the attribute contribution matrices  $W_s$  and  $W_t$  are also refined, both of them have  $N_p$  rows. The source projection matrix  $P_s$  is obtained as [2]:

$$\begin{aligned} \min_{P_s} \frac{1}{N_p} \sum_{i=1}^{N_p} \|W_t - W_s \cdot P_s\|_2^2 + \sum_{i=1}^{d_t} \lambda \|P_{s_i}\|_1 \\ \text{such that } P_{s_i} \geq 0 \end{aligned} \quad (1)$$

Using  $P_s$ , SHDA calculates the projected source data ( $D_s \times P_s$ ) which are then appended to  $D_t$  to build the final classifier. It is reported that SHDA outperforms existing state-of-the-art methods [2]. However, since SHDA projects the whole  $D_s$  into  $D_t$ , the final classifier may suffer from negative transfer resulting in a low classification accuracy if the number of pivots between  $D_s$  and  $D_t$  is very low.

The existing methods therefore have room for further improvement. TLF, is capable of transferring knowledge from  $D_s$  and  $D_t$  by using dynamic distribution adaptation (DDA) and manifold regularization (MR) even if  $d_s \neq d_t$ ,  $Y_s \neq Y_t$  and  $n_s \gg n_t$ . A comparison on the properties of TLF and some existing methods is presented in Table 3.

#### 4. Proposed Framework TLF

The motivation of TLF is presented in the introduction section. We now present our proposed a novel framework called TLF for supervised heterogeneous transfer learning (HTL). We then analyze the target domain error bound and computational complexity of TLF.



Table 3: Comparison of TLF and some existing methods, where DDA and MR denote dynamic distribution adaptation and manifold regularization, respectively.

Method [Ref.]	DDA?	MR?	$d_s \neq d_t$ ?	$Y_s \neq Y_t$ ?	$n_s \gg n_t$ ?
DASVM [5]	No	No	No	No	No
ARTL [3]	No	Yes	No	No	No
MEDA [4]	Yes	Yes	No	No	No
BDA [16]	Yes	Yes	No	No	No
SHDA [2]	No	No	Yes	Yes	Yes
<b>TLF [ours]</b>	Yes	Yes	Yes	Yes	Yes

#### 4.1. General Framework

TLF consists of five main steps as follows (also shown in Algorithm 1).

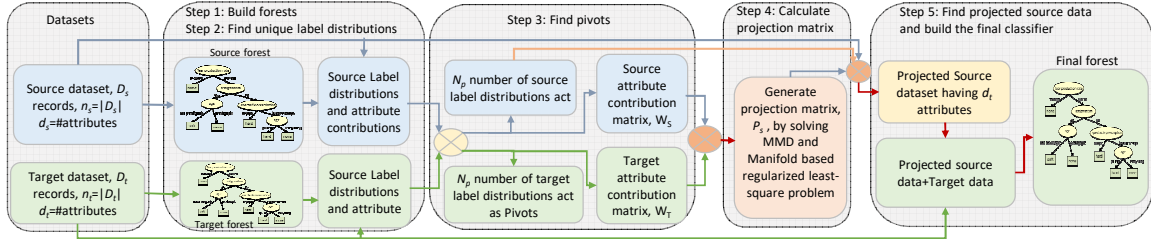


Figure 4: Overall flow diagram of our proposed transfer learning framework, TLF.

**Step-1:** Build forests and find label distributions and centroids from both source  $D_s$  and target  $D_t$  domains.

**Step-2:** Remove duplicate label distributions and find the aggregated values of the corresponding centroids.

**Step-3:** Find pivots between source and target domains.

**Step-4:** Calculate projection matrix between source and target domains.

**Step-5:** Find and transfer projected source data to the target domain and build the final classifier.

We also present an overall flow diagram of TLF as shown in Fig. 4. We now discuss the steps as follows.

**Step-1: Build forests and find label distributions and centroids from both source  $D_s$  and target  $D_t$  domains.**

In TLF, we take two datasets, namely source domain dataset  $D_s$  and target dataset  $D_t$  as input.  $D_s$  has  $n_s$  rows,  $d_s$  attributes and  $C_s$  labels, and  $D_t$  has  $n_t$  rows,  $d_t$  attributes and  $C_t$  labels. In this step, we build two forests  $F_s$  and  $F_t$  (where each forest has  $\tau$  trees) by applying a decision forest algorithm such as Random Forest (RF) [15] on  $D_s$  and  $D_t$ , respectively as shown in the Step 1 of Algorithm 1 and Fig. 4. Using  $F_s$ , we find the leaves  $L_s$  (see Fig. 3) where a leaf  $l_s^i \in L_s$  is represented by the  $i$ th

rule of  $F_s$ . For the  $i$ th leaf  $l_s^i$ , we find records (from  $D_s$ ) that belong to  $l_s^i$ . We then calculate the label distribution  $v_s^i$ , the centroid  $w_s^i$  and centroid's label  $r_s^i \in C_s$ . The  $v_s^{ij}$  is the probability of the  $j$ th label in  $l_s^i$ . If the  $j$ th attribute is a numerical attribute then the value of  $w_s^{ij}$  is calculated as follows.

$$w_s^{ij} = u_s^{ij} + \log(std) \quad (2)$$

where  $u_s^{ij}$  and  $std$  are the  $j$ th attribute mean and standard deviation, respectively, of the records that belong to leaf  $l_s^i$ . For categorical attributes, we use the mode values. Thus, for all leaves of  $F_s$  we obtain a label distribution matrix  $V_s^{[L_s \times C_s]}$ , a centroid matrix  $W_s^{[L_s \times d_s]}$  and a matrix for centroids label  $R_s^{[L_s \times 1]}$ . Similarly, using  $D_t$  and  $F_t$ , we find a label distribution matrix  $V_t^{[L_t \times C_t]}$ , a centroid matrix  $W_t^{[L_t \times d_t]}$  and a matrix for centroids label  $R_t^{[L_t \times 1]}$ . The centroids are considered as the attribute contributions which are calculated differently than SHDA [2].

**Step-2: Remove duplicate label distributions and find the aggregated values of the corresponding centroids.**

Since label distribution of a leaf is calculated based on the number of records, of each label, belonging to the leaf, the existence of duplicate label distributions at the leaves is common. For example, Leaf 2 and Leaf 4 of the sample tree (in Fig. 3) have the same label distribution. In this step, we remove duplicates from  $V_s$  and  $V_t$  as shown in Step 2 of Algorithm 1. For every duplicate entry in  $V_s$  and  $V_t$ , the corresponding centroids in  $W_s$  and  $W_t$  are aggregated. For numerical and categorical attributes we take the average and mode values, respectively. This procedure helps to keep attribute contributions for the aggregated vectors. Let  $L'_s$  and  $L'_t$  be the number of entries remained after the aggregation. Now, the matrices are:  $V_s^{[L'_s \times C_s]}$ ,  $V_t^{[L'_t \times C_t]}$ ,  $W_s^{[L'_s \times d_s]}$ ,  $W_t^{[L'_t \times d_t]}$ ,  $R_s^{[L'_s \times 1]}$  and  $R_t^{[L'_t \times 1]}$ .

**Step-3: Find pivots between source and target domains.**

In most real-world HTL scenarios, the feature discrepancy is a challenging issue since the correspondences between  $D_s$  and  $D_t$  are not available. To minimize the discrepancy, some common information between  $D_s$  and  $D_t$  can be identified to bridge the domains. Since we assume that both  $D_s$  and  $D_t$  share some label space, we exploit the shared label space to identify correspondences between domains. Thus, in Step 3, we determine the leaves with similar label distributions across the domains as shown in Step 3 of Algorithm 1 and Fig. 4.

Let  $S^{L'_s \times L'_t}$  be the similarity matrix of  $V_s^{[L'_s \times d_s]}$  and  $V_t^{[L'_t \times d_t]}$ , where each value varies between 0

and 1. A lower value indicates a higher similarity. The similarity of two label distributions is computed using the Jensen Shannon divergence (JSD) method [17]. A source label distribution  $V_s^i$  is said to be similar to a target label distribution  $V_t^k$  if the divergence between them is less than 10%.

Since  $D_t$  generally contains small labeled data, it is common to have a small number of common labels. So, we may have only a small number of similar labeled distributions across the domains. Each shared labeled distribution (i.e.  $(V_s^i, V_t^k)$ ) is considered as a pivot that acts as the bridge between  $D_s$  and  $D_t$ . Let  $N_p$  be the number of pivots between  $D_s$  and  $D_t$ .

For each pivotal label distribution, we also have the attribute contribution which is calculated in Step 1 and refined in Step 2. Based on the similar source and target label distributions, we then determine the attribute contribution matrices  $W_s^{[N_p \times d_s]}$  and  $W_t^{[N_p \times d_t]}$ , and the associated label matrices  $R_s^{[N_p \times 1]}$  and  $R_t^{[N_p \times 1]}$ .

---

**Algorithm 1: LearnTLF()**

---

**Input** : Source dataset  $D_s$ , target dataset  $D_t$ .  
**Output** : Classifier  $F$ .

**Step 1:**  
 Build two decision forests  $F_s$  and  $F_t$  by applying an existing decision forest algorithm such as RF [15] on  $D_s$  and  $D_t$ , respectively, where  $|F_s|=|F_t|=\tau$  trees;  
 Find source leaves,  $L_s \leftarrow \text{findLeaves}(F_s)$ ;  
 Find source label distributions,  $V_s \leftarrow \text{findClassDistribution}(D_s, L_s)$ ;  
 Find source centroids,  $W_s \leftarrow \text{findCentroids}(D_s, L_s)$ ;  
 Find source centroid's labels,  $R_s \leftarrow \text{findCentroidLabel}(D_s, L_s)$ ;  
 Find target leaves,  $L_t \leftarrow \text{findLeaves}(F_t)$ ;  
 Find target label distributions,  $V_t \leftarrow \text{findClassDistribution}(D_t, L_t)$ ;  
 Find target centroids,  $W_t \leftarrow \text{findCentroids}(D_t, L_t)$ ;  
 Find target centroid's labels,  $R_t \leftarrow \text{findCentroidLabel}(D_t, L_t)$ ;  
**end**

**Step 2:**  
 Remove duplicates from  $V_s$  and  $V_t$ . For every duplicate entry in  $V_s$  and  $V_t$ , the corresponding centroids in  $W_s$  and  $W_t$ , and centroid labels  $R_s$  and  $R_t$  are aggregated.  
**end**

**Step 3:**  
 Calculate similarity matrix,  $S \leftarrow \text{calculateSimilarityByJSD}(V_s, V_t)$  between source and target label distributions;  
 Find source pivots,  $V_s \leftarrow \text{findPivots}(V_s, S)$  and associated centroids  $W_s$  and labels  $R_s$ ;  
 Find target pivots,  $V_t \leftarrow \text{findPivots}(V_t, S)$  and associated centroids  $W_t$  and labels  $R_t$ ;  
**end**

**Step 4:**  
 Find projection matrix,  $P_s \leftarrow \text{findProjectionMatrix}(W_s, R_s, W_t, R_t)$  by considering ridge, maximum mean discrepancy (MMD) and manifold regularizations as shown in Eq. (22)  
**end**

**Step 5:**  
 Find transferrable source data,  $D'_s \leftarrow \text{findProjectedSourceData}(V_s, D_s, P_s)$ ;  
 Projected source data,  $D''_s \leftarrow D'_s \times P_s$ ;  
 New target dataset,  $D'_t \leftarrow \text{merge}(D''_s, D_t)$ ;  
 Build the final decision forest,  $F$  by applying the RF on  $D'_t$ ;  
 Return  $F$ .  
**end**

---

**Step-4: Calculate projection matrix between source and target domains.**

In this step, we calculate a projection matrix  $P_s$  for  $D_s$  so that the data can be projected to  $D_t$  as shown in Step 4 of Algorithm 1 and Fig. 4. We calculate  $P_s$  by applying structural risk minimization (SRM) principle and regularization theory [14] on the attribute contribution matrices  $W_s^{[N_p \times d_s]}$  and  $W_t^{[N_p \times d_t]}$ . Let  $J_s$  and  $J_t$  be the source and target joint probability distributions, respectively and  $P_s$  and  $P_t$  be the source and target marginal distributions, respectively. To calculate  $P_s$  we particularly, aim to optimize the following three objective functions:

1. To minimize structural risk function on  $W_s$  and  $W_t$ ;
2. To minimize distribution discrepancy between  $J_s$  and  $J_t$ ; and
3. To maximize manifold consistency underlying  $P_s$  and  $P_t$ .

Let  $D_c$  be the combine dataset of  $(W_s, R_s)$  and  $(W_t, R_t)$  i.e.  $D_c = \{(w_{s_1}, r_{s_1}), \dots, (w_{s_{N_p}}, r_{s_{N_p}}), (w_{t_1}, r_{t_1}), \dots, (w_{t_{N_p}}, r_{t_{N_p}})\}$ . By ignoring source and destination subscripts, we can simply write  $D_c$  as  $\{(w_1, r_1), \dots, (w_z, r_z)\}$ , where  $z = 2N_p$ . Also let  $f = \beta^T \phi(w)$  be the classifier having parameters  $w$  and feature mapping function  $\phi : w \mapsto \mathcal{H}$  that projects the actual feature vector to a Hilbert space  $\mathcal{H}$ . Using the SRM principle and regularization theory, the framework of TLF can be formulated as:

$$f = \operatorname{argmin}_{f \in \mathcal{H}_K} \sum_{i=1}^z l(f(w_i), r_i) + \sigma \|f\|_K^2 + \lambda D_{f,K}(J_s, J_t) + \gamma M_{f,K}(P_s, P_t) \quad (3)$$

where  $K$  is the kernel function represented by  $\phi$  such that  $\langle \phi(w_i), \phi(w_j) \rangle = K(w_i, w_j)$ , and  $l(\cdot, \cdot)$ ,  $\|f\|_K^2$  and  $D_{f,K}(\cdot, \cdot)$  represent loss function, ridge regularization and dynamic distribution adaptation (DDA), respectively. Moreover, we introduce  $M_{f,K}(P_s, P_t)$  as a Laplacian regularization to further exploit intrinsic properties of nearest points in Manifold  $\mathcal{G}$  [9]. The symbols  $\sigma$ ,  $\lambda$ , and  $\gamma$  are positive regularization parameters for ridge, DDA, and Manifold, respectively.

In Eq. (3), the loss function  $l(\cdot)$  measures the fitness of  $f$  for classifying labels on  $D_c$ . We use SVM [14] to solve  $l(\cdot)$ . Moreover, since the kernel mapping  $\phi : w \mapsto \mathcal{H}$  may have infinite dimensions, we solve Eq. (3) by reformulating it with the following Representer Theorem.

**Theorem 1.** (*Representer Theorem*) [3, 14] *If  $K$  is a kernel function induced by  $\phi$  then the optimization problem in Eq. (3) for  $D_c$ , can be represented by*

$$f(w) = \sum_{i=1}^z \alpha_i K(w_i, w) \text{ and } \beta = \sum_{i=1}^z \alpha_i \phi(w_i) \quad (4)$$

where  $\alpha_i$  is a coefficient.

Using the SRM principle and equations (4), we can reformulate loss function, ridge regularization of Eq. (3) as follows.

$$f = \underset{f \in \mathcal{H}}{\operatorname{argmin}} \left\| R - \alpha^T K \right\|_F^2 + \sigma(\operatorname{tr}(\alpha^T K \alpha)) \quad (5)$$

We now discuss the process of minimizing distribution divergence through dynamic distribution adaptation and manifold regularization as follows.

**Dynamic Distribution Adaptation (DDA):** Since the joint distributions  $J_s$  and  $J_t$  are different, the loss function  $l(\cdot)$  with only the ridge regularization in Eq. (3) may not generalize well to  $W_t$  [3]. Thus, we aim to minimize joint distribution divergence 1) between the marginal distributions  $P_s$  and  $P_t$ , and 2) between the conditional distributions  $Q_s$  and  $Q_t$ , simultaneously.

Following ARTL [3] and MEDA [4], we adopt MMD [8] to handle the distribution divergence. Based on the samples drawn from two domains, MMD is capable of determining whether two distributions are different or not. The MMD between marginal distributions  $P_s$  and  $P_t$  is computed as

$$\operatorname{MMD}_{\mathcal{H}}^2(W_s, W_t) = \left\| \frac{1}{N_p} \sum_{i=1}^{N_p} \phi(w_i) - \frac{1}{N_p} \sum_{j=N_p+1}^{N_p+z} \phi(w_j) \right\|_{\mathcal{H}}^2 \quad (6)$$

where  $\phi : w \mapsto \mathcal{H}$  is a feature mapping. The MMD can be regularized for the classifier  $f$  as

$$D_{f,K}(P_s, P_t) = \left\| \frac{1}{N_p} \sum_{i=1}^{N_p} f(w_i) - \frac{1}{N_p} \sum_{j=N_p+1}^{N_p+z} f(w_j) \right\|_{\mathcal{H}}^2 \quad (7)$$

where  $f = \beta^T \phi(w)$ .

Since we have labeled data in both domains, we now minimize the distance  $D_{f,K}(P_s, P_t)$  between conditional distributions  $Q_s$  and  $Q_t$ . Based on the intra-class centroids of two distributions  $Q_s(w_s|r_s)$  and  $Q_t(w_t|r_t)$ , the MMD of a class  $c \in C$  is computed as

$$D_{f,K}^{(c)}(Q_s, Q_t) = \left\| \frac{1}{|W_s^{(c)}|} \sum_{w_i \in W_s^{(c)}} f(w_i) - \frac{1}{|W_t^{(c)}|} \sum_{w_j \in W_t^{(c)}} f(w_j) \right\|_{\mathcal{H}}^2 \quad (8)$$

where  $W_s^{(c)} = \{w_i : w_i \in W_s \wedge r(w_i) = c\}$  is the set records associated to class  $c$  in  $D_s$  and  $W_t^{(c)} = \{w_j : w_j \in W_t \wedge r(w_j) = c\}$  is the set records associated to class  $c$  in  $D_t$ . If  $|W_k^{(c)}| = 0$  then we ignore the part of  $|W_k|$  in Eq. (8).

In real-world scenarios, the importance of marginal ( $P$ ) and conditional ( $Q$ ) are different [4]. Thus, the divergence for joint joint distributions  $J_s$  and  $J_t$  is adapted dynamically by integrating Eq. (7) and Eq. (8) as follows.

$$D_{f,K}(J_s, J_t) = (1 - \mu)D_{f,K}(P_s, P_t) + \mu \sum_{c=1}^C D_{f,K}^{(c)}(Q_s, Q_t) \quad (9)$$

where  $\mu \in [0, 1]$  is the adaptive factor which is calculated dynamically by following MEDA [4].  $\mu \rightarrow 0$  indicates the distribution distance between the domains is large, and thus, the marginal distribution adaptation is important. Besides,  $\mu \rightarrow 1$  indicates the class distribution is dominant than feature distribution, and thus, the conditional distribution adaptation is important.

Using the Representer Theorem (see Theorem 1 and Eq. (4)), Eq. (9) becomes

$$D_{f,K}(J_s, J_t) = \text{tr}(\alpha^T K M K \alpha) \quad (10)$$

where  $M^{[z \times z]} = (1 - \mu)M_0 + \mu \sum_{c=1}^C M_c$  is the MMD matrix. The components of the MMD matrix are calculated as follows.

$$(M_0)_{ij} = \begin{cases} \frac{1}{N_p^2} & w_i, w_j \in W_s \vee w_i, w_j \in W_t \\ \frac{-1}{N_p^2} & \text{otherwise} \end{cases}; \forall i, j \quad (11)$$

$$(M_c)_{ij} = \begin{cases} \frac{1}{n_c^2} & w_i, w_j \in W_s^{(c)} \\ \frac{1}{m_c^2} & w_i, w_j \in W_t^{(c)} \\ \frac{-1}{n_c^2 m_c^2} & w_i, w_j \in W_s^{(c)} \vee w_i, w_j \in W_t^{(c)} \\ 0 & \text{otherwise} \end{cases} ; \forall i, j \quad (12)$$

where  $n_c = |W_s^{(c)}|$  and  $m_c = |W_t^{(c)}|$ .

**Manifold Regularization:** In addition to DDA, we further exploit intrinsic properties of the marginal distributions  $P_s$  and  $P_t$  by manifold regularization [9] due to its effectiveness in mitigating influence of feature distortion [3, 4]. The features of a domain can be transformed into manifold space which is suitable for exploiting more detailed property and structure of the domain. Considering the manifold assumption [9], the manifold regularization is computed as

$$\begin{aligned} M_{f,K}(P_s, P_t) &= \sum_{i,j=1}^z (f(w_i) - f(w_j))^2 B_{ij} \\ &= \sum_{i,j=1}^z f(w_i) L_{ij} f(w_j) \end{aligned} \quad (13)$$

where  $L^{[z \times z]}$  is the normalized Laplacian regularization matrix and  $B$  is the graph affinity matrix which is calculated as

$$B_{ij} = \begin{cases} \cos(w_i, w_j) & \text{if } w_i \in k(w_j) \vee w_j \in k(w_i) \\ 0 & \text{otherwise} \end{cases} \quad (14)$$

where  $\cos(., .)$  is a similarity function which is used to calculate distance between two records  $w_i$  and  $w_j$ , and  $k(w_j)$  represents the  $k$  nearest-neighbors (kNN) of the record  $w_j$ . While existing methods including ARTL [3] and MEDA [4] use a user-defined value for  $k$ , we propose a novel approach to determine  $k$  automatically so that the intrinsic properties of a record can be exploited more accurately resulting in a high transfer performance.

In TLF, we determine  $k$  NN of a record  $w_i$  having label  $r_i$  as follows. We first calculate distance between  $w_i$  and other records one by one and then sort the records based on the distance in ascending

order. We set the minimum of value of  $k$  to 4. That is, the first four records are added to kNN set. Following the order, we continue to add a record  $w_u$  to kNN set iteratively until  $r_i \neq r_u; \forall u$ . Fig. 5 illustrates the difference between user-defined and automatic  $k$ , the automatic one finds the nearest-neighbors of a record more accurately.

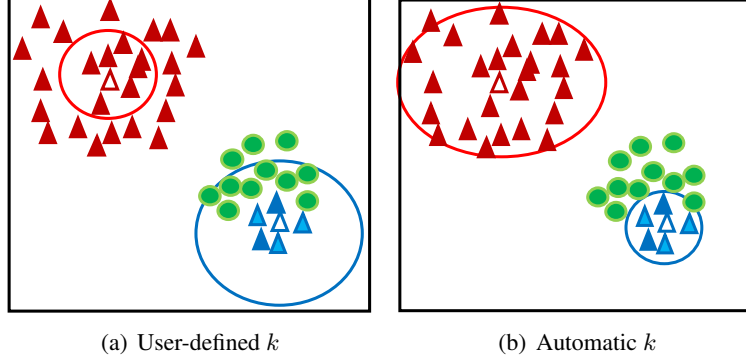


Figure 5: Justification of determining  $k$  value automatically in manifold regularization.

We test the influences of automatic  $k$  on a real-world dataset Reuters-215782 (RT) [18] which has 3 cross-domain pairs as follows:  $\text{orgs} \mapsto \text{people}$ ,  $\text{orgs} \mapsto \text{place}$  and  $\text{people} \mapsto \text{place}$  (see Section 5.1 for details). We first apply TLF on each pair for different user-defined  $k$  values such as 4, 8, 16, 32 and 64, and then calculate classification accuracy for each  $k$ . After that we apply TLF on each pair where  $k$  is determined automatically and then calculate classification accuracy. We present the results of the pairs in Fig. 6. The figure clearly shows the effectiveness of automatic  $k$  since TLF achieves the best results when we determine  $k$  automatically.

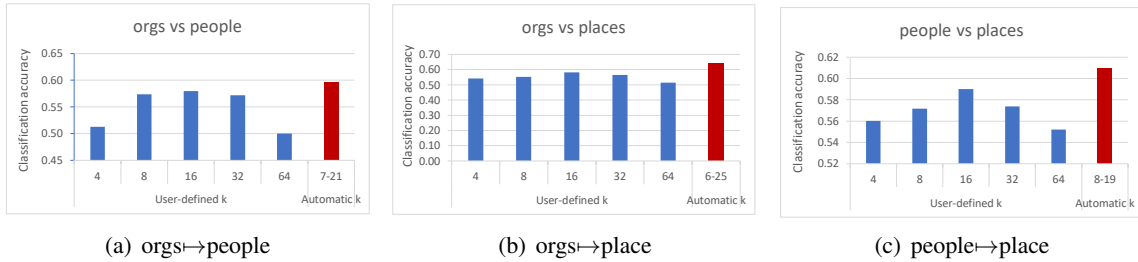


Figure 6: Justification of automatic determination of  $k$  value on RT dataset in terms of classification accuracy.

The Laplacian matrix,  $L$  of Eq. (13) is calculated as

$$L = I - D^{-\frac{1}{2}} B D^{-\frac{1}{2}} \quad (15)$$



where  $D$  is a diagonal matrix with each element  $D_{ii} = \sum_{j=1}^z B_{ij}$ . Thus, by incorporating Eq. (4) into Eq. (13), we get

$$M_{f,K}(P_s, P_t) = \text{tr}(\alpha^T K L K \alpha) \quad (16)$$

Using equations (5), (10) and (16), we can reformulate  $f$  in Eq. (3) as follows.

$$f = \underset{f \in \mathcal{H}}{\text{argmin}} \left\| R - \alpha^T K \right\|_F^2 + \sigma(\text{tr}(\alpha^T K \alpha)) \quad (17)$$

$$+ \lambda(\text{tr}(\alpha^T K M K \alpha)) + \gamma(\text{tr}(\alpha^T K L K \alpha)) \quad (18)$$

Setting derivative  $\frac{\partial f}{\partial \alpha} = 0$ , we obtain the solution as

$$\alpha = \sigma I + (\lambda M + \gamma L) K \quad (19)$$

We now transform the attribute contribution matrices  $W_s^{[N_p \times d_s]}$  and  $W_t^{[N_p \times d_t]}$  into  $G_s^{[z \times d_s]}$  and  $G_t^{[z \times d_t]}$ , respectively as follows.

$$(G_s)_{ij} = \begin{cases} e_{ij} & \text{if } e_{ij} = w_{ij} \wedge w_i \in W_s \\ 0 & \text{otherwise} \end{cases} ; \forall i, j \quad (20)$$

$$(G_t)_{ij} = \begin{cases} e_{ij} & \text{if } e_{ij} = w_{ij} \wedge w_i \in W_t \\ 0 & \text{otherwise} \end{cases} ; \forall i, j \quad (21)$$

Using equations (19), (20) and (21), we obtain the projection matrix  $P_s$  as follows.

$$P_s = G_s^T \alpha G_t \quad (22)$$

**Step-5: Find and transfer projected source data to the target domain and build the final classifier.**

In this step, we first identify transferable data  $D'_s$  from  $D_s$  by using the projection matrix  $P_s$  (obtained in Eq. (22)) and source pivots  $V_s$  (obtained in Step 3). We then project  $D'_s$  into  $D''_s$  i.e.  $D''_s = D'_s \times P_s$ . After that we merge  $D''_s$  with  $D_t$  and obtain  $D'_t$  (see Step 5 of Algorithm 1 and Fig. 4). We finally build the final forest  $F$  by applying RF on  $D'_t$ . The final classifier is then used to classify unlabeled target data.

#### 4.2. Generalization Bound Analysis

Following the approaches in [3, 4, 19], we analyze the generalization error bound of TLF on the target domain based on the structural risk on the source domain. Let  $y = h(x)$  and  $\hat{y} = f(x)$  be the true labeling function and prediction function, respectively. Also let  $l(x)$  be a continuous loss function  $l(x) = |h(x) - f(x)|$  and  $e$  be the expected error  $e = l(x)$ . The expected error  $e_t(f)$  of the prediction function  $f(x)$ , where a record  $x$  is drawn from the target domain  $D_t$ , is defined as

$$e_t(f) = E_{x \sim p_t} [|h(x) - f(x)|] = E_{x \sim p_t} [l(x)] \quad (23)$$

Similarly, the expected error  $e_s(f)$  of the prediction function  $f(x)$ , where a record  $x$  is drawn from the source domain  $D_s$ , is defined as

$$e_s(f) = E_{x \sim p_s} [|h(x) - f(x)|] = E_{x \sim p_s} [l(x)] \quad (24)$$

Let  $\hat{e}_s(f)$  and  $\hat{e}_t(f)$  be the empirical errors of  $f$  in  $D_s$  and  $D_t$ , respectively and  $\hat{e}(f) = \hat{e}_s(f) + \hat{e}_t(f)$  be the total empirical error of both  $D_s$  and  $D_t$ . Following the approaches in [3, 19], now we present the error bound for the target domain in terms of the source risk in Theorem 2.

**Theorem 2.** [3, 19] *If  $d$  be the Vapnik-Chervonenkis (VC) dimension [14] of a prediction function  $f$  for the target domain  $D_t$  then the expected error  $e_t(f)$  of  $f$  in  $D_t$  is bounded with probability at least*

$1 - \delta$  by

$$e_t(f) \leq \hat{e}_s(f) + \sqrt{\frac{4}{n} \left( d \cdot \log\left(\frac{2 \cdot e \cdot n}{d}\right) + \log\left(\frac{4}{\delta}\right) \right)} \quad (25)$$

$$+ D_{f,K}(J_s, J_t) + \Omega \quad (26)$$

where  $n$  is the number of records,  $e$  is the base of natural logarithm and  $\Omega = \inf_{f \in H_K} [e_s(f) + e_t(f)]$ .

*Proof.* Following the VC theory [14], the expected error  $e_s(f)$  of  $f$  in  $D_s$  for a VC dimension  $d$  is bounded with high probability  $1 - \delta$  by

$$e_s(f) \leq \hat{e}_s(f) + \sqrt{\frac{4}{n} \left( d \cdot \log\left(\frac{2 \cdot e \cdot n}{d}\right) + \log\left(\frac{4}{\delta}\right) \right)} \quad (27)$$

Now we can write Eq. (23) as

$$e_t(f) = E_{x \sim p_t} [l(x)] \quad (28)$$

By adding an error term  $\hat{e}_t(f) \geq 0$ , Eq. (28) can be expressed as

$$\begin{aligned} e_t(f) &\leq \hat{e}_t(f) + E_{x \sim p_t} [l(x)] \\ &\leq \hat{e}_t(f) + E_{x \sim p_s} [l(x)] + [E_{x \sim p_t} [l(x)] - E_{x \sim p_s} [l(x)]] \end{aligned} \quad (29)$$

Again, let  $D_{f,K}(J_s, J_t)$  be the distribution difference between the joint probability distributions  $J_s$  and  $J_t$ , where  $D_{f,K}(J_s, J_t) = [E_{x \sim p_t} [l(x)] - E_{x \sim p_s} [l(x)]]$ . Thus, Eq. (29) can be expressed as

$$\begin{aligned} e_t(f) &\leq \hat{e}_t(f) + E_{x \sim p_s} [l(x)] + D_{f,K}(J_s, J_t) \\ &\leq \hat{e}_t(f) + \hat{e}_s(f) + e_s(f) + D_{f,K}(J_s, J_t) \\ &\leq \Omega + e_s(f) + D_{f,K}(J_s, J_t) \end{aligned} \quad (30)$$

Thus by substituting the value of  $e_s(f)$  from Eq. (27), Eq. (30) can be expressed as

$$e_t(f) \leq \hat{e}_s(f) + \sqrt{\frac{4}{n} \left( d \cdot \log\left(\frac{2 \cdot e \cdot n}{d}\right) + \log\left(\frac{4}{\delta}\right) \right)} \quad (31)$$

$$+ D_{f,K}(J_s, J_t) + \Omega \quad (32)$$

□

From Theorem 2, the expected error  $e_t(f)$  in  $D_t$  is bounded if we can simultaneously minimize 1) the empirical error of labeled data in  $D_s$ , i.e.,  $\hat{e}_s(f)$ , 2) the distribution distance between  $D_s$  and  $D_t$  in  $\mathcal{H}$ , i.e.,  $D_{f,K}(J_s, J_t)$ , and 3) the adaptability of the true function  $h$  in terms of hypothesis space  $H_K$ , i.e.,  $\Omega$ .

In TLF framework, i.e., Eq. (3),  $\hat{e}_s(f)$  is explicitly minimized by structural risk minimization in Eq. (5);  $D_{f,K}(J_s, J_t)$  is explicitly minimized by distribution adaptation in Eq. (10);  $\Omega$  is implicitly minimized by manifold regularization in Eq. (16).

#### 4.3. Computational Complexity

We now calculate the complexity of TLF (as shown in Algorithm 1). As input, TLF takes two datasets:  $D_s$  has  $n_s$  records and  $d_s$  attributes, and  $D_t$  has  $n_t$  records and  $d_t$  attributes. Let  $D_s$  and  $D_t$  have  $C$  common labels and  $n(= n_s + n_t)$  records.

In Step 1, we build two forests  $F_s$  and  $F_t$  having  $\tau$  trees each. Since  $n_s \gg n_t$ , the complexity of building forests is  $O(\tau d_s n_s^2 \log(n_s))$  [2]. We then identify shared label distributions that has a complexity  $O(\tau^2 n_s n_t C)$ .

The complexity of Step 2 is  $C(l_s^2 + l_t^2)$  where  $l_s$  and  $l_t$  are the leaves of  $F_s$  and  $F_t$ , respectively. In Step 3,  $N_p$  common label distributions across the domains are identified. The complexity of Step 3 is  $O(N_p(d_s + d_t))$ .

The complexity of Step 4 consists of three parts: (i) solving the linear system of Eq. (5) using LU decomposition that has a complexity  $O((z)^3)$  [3] for TLF, where  $z = 2N_p$ , (ii) for constructing the graph Laplacian matrix  $L$ , TLF needs  $O((d_s + d_t)z^2)$ , which is performed once, and (iii) for constructing the kernel matrix  $K$  and aggregate MMD matrix  $M$ , TLF requires  $O(Cz^2)$ . In Step 5, TLF needs  $O(n_s d_s d_t)$  for transferring the source dataset to target domain. Finally, in Step 6, TLF builds the final decision forest which requires  $O(\tau d_t n^2 \log(n))$ . Typically,  $n_t$ ,  $N_p$ ,  $C$ ,  $z$ ,  $l_s$  and  $l_t$

are very small, especially compared to  $n$ . Therefore, the overall complexity of TLF is  $O(n_s d_s d_t + \tau d_t n^2 \log(n))$ .

## 5. Experiments

### 5.1. Data Preparation

We apply TLF and eleven existing methods on seven real datasets which are shown at a glance in Table 4.

Table 4: datasets at a glance.

dataset [Ref.]	#Records	#Attributes	#Classes	Sub-domain	Area
PIE [20]	11554	1024	68	PIE5, PIE7, PIE9, PIE27, PIE29	Face recognition
Office+Caltech (OC) [20]	2533	800	10	amazon, Caltech10, dslr, webcam	Object recognition
20-Newsgroups (NG) [18]	40252	10000	2	C, S, R, T	Text Classification
VLSC [20]	18070	4096	5	C, I, L, S, V	Image classification
Reuters-21578 (RT) [18]	6570	4000	3	Orgs, People, Places	Text Classification
MNIST+USPS (MU) [20]	3800	256	10	MUS, MUT, UMS, UMT	Object recognition
COIL20 (COIL) [20]	1440	1024	20	C1S, C1T, C2S, C2T	Object recognition

PIE [20] has 11554 handwritten digits from 5 different subcategories: PIE5, PIE7, PIE9, PIE27 and PIE29. We generate 20 combinations of source-target pairs as follows: PIE5 $\mapsto$ PIE7, PIE5 $\mapsto$ PIE9, PIE5 $\mapsto$ PIE27, PIE5 $\mapsto$ PIE29, PIE7 $\mapsto$ PIE5, and so on (see Table 5).

Office+Caltech (OC) [20] has 4 different subcategories: amazon, Caltech10, dslr and webcam. We generate 12 combinations of source-target pairs as follows: amazon $\mapsto$ Caltech10, amazon $\mapsto$ dslr, amazon $\mapsto$ webcam, Caltech10 $\mapsto$ amazon, and so on (see Table 6). 20-Newsgroups (NG) [18] has approximately 20,000 documents distributed evenly in 4 different subcategories: C, S, R, and T. Following the approach in ARTL [3], we have 5 combinations of source-target pairs as follows: CS-src (CSS) $\mapsto$ CS-tgt (CST), CT-src (CTS) $\mapsto$ CT-tgt (CTT), RS-src (RSS) $\mapsto$ RS-tgt (RST), RT-src (RTS) $\mapsto$ RT-tgt (RTT) and ST-src (STS) $\mapsto$ ST-tgt (STT) (see Table 6). VLSC [20] consists of 18070 images from 5 different subcategories: Caltech101 (C), ImageNet (I), LabelMe (L), SUN09 (S), and VOC2007 (V). We generate 20 combinations of source-target pairs as follows: Caltech101 $\mapsto$ ImageNet, Caltech101 $\mapsto$ LabelMe, Caltech101 $\mapsto$ SUN09, Caltech101 $\mapsto$ VOC2007, ImageNet $\mapsto$ Caltech101, and so on (see Table 6).

Similarly, MNIST+USPS (MU) and COIL [20] have 4 different subcategories from which we generate 12 combinations of source-target pairs, separately (see Table 6). Besides, Reuters-215782

(RT) [18] has three top categories orgs, people, and place. Following the approach in ARTL [3], we can construct 3 cross-domain pairs as follows: orgs $\rightarrow$ people, orgs $\rightarrow$ place and people $\rightarrow$ place (see Table 7).

## 5.2. Experimental Setup

### 5.2.1. Target and Test datasets Preparation

From each source $\rightarrow$ target pair, we use the (original) target dataset to create test dataset to evaluate the performance of TLF and existing methods. We divide the (original) target dataset into 2 datasets, namely (new) target and test datasets. Since TLF assumes small labeled data in the target domain, the newly created target and test datasets contain 5% and 95% of records, respectively, of the original target dataset. The size of the target dataset is determined based on empirical evaluation on VLSC and COIL datasets.

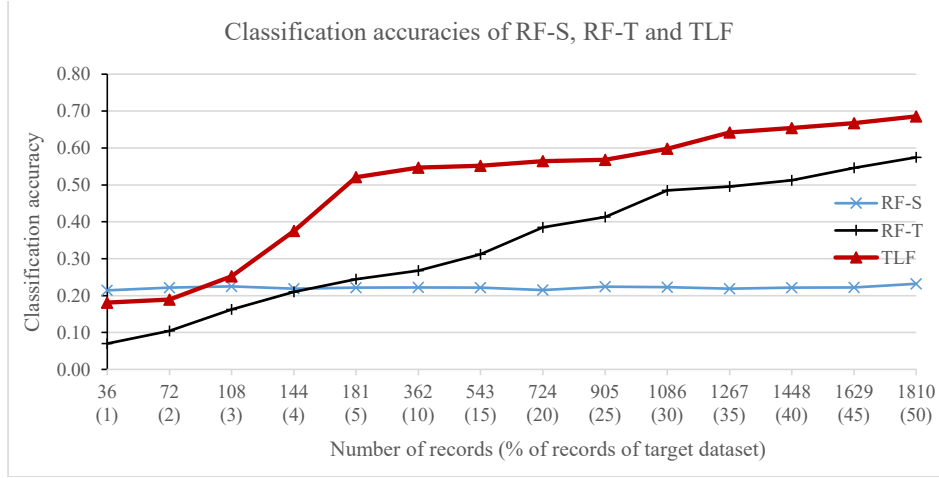
For instance, Fig. 7 shows the classification accuracies of RF-S, RF-T and TLF on VLSC and COIL dataset. For RF-S, we build a forest by applying RF on the source data and use the forest to classify the test data. Similarly, for RF-T, we build a forest by applying RF on the target data and use the forest to classify the test data. The x-axis of the figure shows the size of new target dataset and corresponding ratio (% of records) of the original target dataset.

We can see from Fig. 7a that when target dataset size is 50% (i.e. 1810 records), both TLF and RF-T perform well indicating that the (new) target dataset is sufficient to build a good forest. On the other hand, none of them perform well when the target dataset size is less than 5%. It is worth noting from the figure that a model does not perform well when it is built on the source dataset only. The empirical evaluation clearly demonstrates the need for transfer learning across domains. Therefore, we choose 5% and 95% (of original target dataset) as the size of (new) target and test datasets, respectively to evaluate the techniques properly. We also get similar results on the COIL dataset as shown in Fig. 7b.

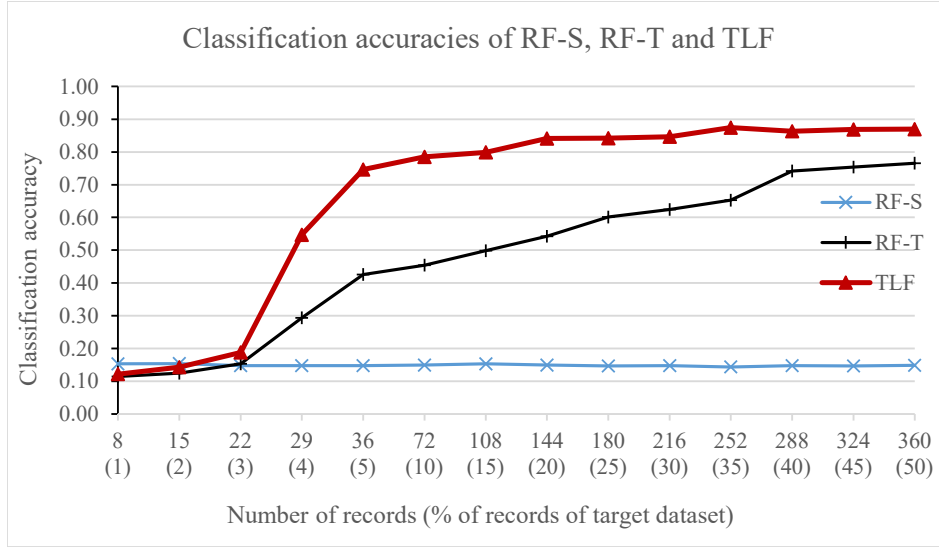
### 5.2.2. Baseline Methods

We compare the performance of TLF with eleven state-of-the-art machine learning and transfer learning techniques, comprising nine transfer learning and two baseline (non-transfer learning) algorithms, namely SHDA [2], MEDA [4, 21], TCA [22], BDA [16], CORAL [23], EasyTL [6], JDA [24], ARTL [3], RF [15], and SysFor [25].

We implement TLF in the Java programming language using the Weka APIs [26]. The source code of TLF is available at GitHub (<https://github.com/grahman20/TLF>). We also implement



(a) VLSC dataset



(b) COIL dataset

Figure 7: Justification of target dataset size on COIL and VLSC datasets in terms of classification accuracy.

an existing technique called SHDA [2]. For implementing the RF and SysFor, we use the Java code from the Weka platform [26]. All other methods are already available in the MEDA framework [21]. We use the default settings of the methods while running the experiment.

### 5.2.3. Implementation Details

In our experiment, we use a number of parameters for TLF and existing techniques. Forest algorithms require two common parameters, namely number of trees ( $\tau$ ) and minimum leaf size.  $\tau$  is set to 10 and the minimum leaf size for large datasets (i.e. the size of the dataset is greater than 10000) is set to 50, otherwise it is set to 20. For TLF, we use  $\lambda = 0.01$ ,  $\theta = 5$  and  $\gamma = 0.001$  for manifold,

MMD and ridge regularizations, respectively. In our experimentation we use the majority voting [27] method to calculate final output of a forest. In case of tie, we consider the prediction distribution of class values to break the tie by following the WEKA [26] and MOA [28] approaches.

### 5.3. Experimental Results

We present the performances of TLF and existing methods on 20 pairs of SDD and TDD that are created from PIE dataset in Table 5.

For each method with suffix '-S', we first build a classifier by applying the method on the SDD. We then calculate the classification accuracy by applying the classifier on the test data. For example, for combination 1 ("PIE05→PIE07") the classification accuracy of RF-S is 0.052 which is reported in the first row (under the RF-S column) in Table 5. Similarly, for each method with suffix '-T', we first build a classifier by applying the method on the TDD and then calculate the classification accuracy by applying the classifier on the test data. For example, for combination 1 ("PIE05→PIE07 ") the classification accuracy of RF-T is 0.064 which is reported in the first row (under the RF-T column) in Table 5.

For each transfer learning method, we take both SDD and TDD as input of the method and get a classifier as output. We then calculate the classification accuracy by applying the classifier on the test data. For example, for combination 1 ("PIE05→PIE07 ") the classification accuracy of TLF is 0.338 which is reported in the first row (under the TLF column) in Table 5. Bold values in the table indicate that TLF performs the best in all combinations.

For each method, we also calculate the average classification accuracy from the classification accuracies of 20 combinations as shown in the last row of the table. The average classification accuracy of TLF is 0.472. It is clear from the experimental results that TLF outperforms other techniques on PIE dataset.

Table 6 presents the classification accuracies of TLF and the existing methods on Office+Caltech (OC), 20-Newsgroups (NG) and VLSC datasets. For OC dataset, we present the performances of the techniques of 12 combinations of SDD and TDD in the top 12 rows of the table. Bold values in the table indicate that TLF performs the best in all combinations. For each method, we also calculate the average classification accuracy from the classification accuracies of 12 combinations as shown in the 13-th row of the table. The average classification accuracy of TLF is 0.400. The experimental results clearly indicate that TLF outperforms other methods on OC dataset.



Table 5: Classification accuracies of TLF and existing methods on PIE dataset.

Domains		Baseline methods				Existing transfer learning methods									TLF
Source	Target	RF-S	RF-T	SysFor-S	SysFor-T	EasyTL	ARTL	GFK	TCA	JDA	CORAL	BDA	MEDA	SHDA	
PIE05	PIE07	0.052	0.064	0.025	0.045	0.098	0.265	0.233	0.274	0.214	0.111	0.306	0.269	0.298	<b>0.338</b>
PIE05	PIE09	0.041	0.050	0.023	0.051	0.124	0.378	0.294	0.322	0.265	0.127	0.335	0.282	0.224	<b>0.381</b>
PIE05	PIE27	0.056	0.090	0.024	0.087	0.337	0.540	0.354	0.493	0.236	0.368	0.510	0.485	0.343	<b>0.584</b>
PIE05	PIE29	0.039	0.060	0.015	0.048	0.092	0.172	0.219	0.242	0.214	0.097	0.246	0.174	0.224	<b>0.249</b>
PIE07	PIE05	0.066	0.152	0.022	0.085	0.226	0.321	0.234	0.232	0.265	0.225	0.238	0.219	0.253	<b>0.386</b>
PIE07	PIE09	0.121	0.050	0.037	0.051	0.133	0.492	0.488	0.340	0.265	0.137	0.494	0.427	0.224	<b>0.526</b>
PIE07	PIE27	0.181	0.090	0.080	0.087	0.358	0.482	0.612	0.514	0.377	0.354	0.362	0.484	0.343	<b>0.662</b>
PIE07	PIE29	0.086	0.060	0.022	0.048	0.105	0.327	0.312	0.295	0.215	0.108	0.338	0.271	0.224	<b>0.364</b>
PIE09	PIE05	0.049	0.152	0.046	0.085	0.218	0.323	0.357	0.297	0.265	0.228	0.389	0.224	0.353	<b>0.392</b>
PIE09	PIE07	0.095	0.064	0.051	0.045	0.123	0.428	0.253	0.366	0.356	0.128	0.252	0.434	0.298	<b>0.529</b>
PIE09	PIE27	0.147	0.090	0.104	0.087	0.356	0.533	0.628	0.547	0.451	0.360	0.366	0.536	0.343	<b>0.682</b>
PIE09	PIE29	0.073	0.060	0.054	0.048	0.127	0.325	0.392	0.361	0.315	0.126	0.362	0.331	0.224	<b>0.411</b>
PIE27	PIE05	0.077	0.152	0.025	0.085	0.361	0.538	0.576	0.253	0.526	0.386	0.355	0.480	0.430	<b>0.605</b>
PIE27	PIE07	0.156	0.064	0.057	0.045	0.192	0.590	0.466	0.560	0.652	0.189	0.701	0.591	0.298	<b>0.740</b>
PIE27	PIE09	0.188	0.050	0.082	0.051	0.211	0.666	0.734	0.625	0.457	0.218	0.475	0.664	0.224	<b>0.769</b>
PIE27	PIE29	0.098	0.060	0.043	0.048	0.149	0.438	0.248	0.449	0.365	0.151	0.422	0.374	0.224	<b>0.481</b>
PIE29	PIE05	0.046	0.152	0.020	0.085	0.148	0.212	0.251	0.202	0.215	0.187	0.256	0.126	0.244	<b>0.292</b>
PIE29	PIE07	0.058	0.064	0.021	0.045	0.091	0.253	0.296	0.256	0.251	0.099	0.284	0.257	0.230	<b>0.302</b>
PIE29	PIE09	0.034	0.050	0.022	0.051	0.108	0.280	0.233	0.286	0.214	0.123	0.232	0.284	0.224	<b>0.312</b>
PIE29	PIE27	0.050	0.090	0.022	0.087	0.261	0.312	0.391	0.359	0.322	0.270	0.432	0.319	0.343	<b>0.437</b>
Average		0.086	0.083	0.040	0.063	0.191	0.394	0.379	0.364	0.322	0.200	0.368	0.362	0.278	<b>0.472</b>

The next 5 rows of Table 6 presents the performances of the techniques of 5 combinations of SDD and TDD that are created from the NG dataset. The best performances are indicated with bold values. The table shows that TLF performs the best in all combinations.

We present the performances of the techniques of 20 combinations of SDD and TDD that are created from the VLSC dataset in the last 21 rows of Table 6. For VLSC dataset, TLF performs the best in 15 (out of 20) cases. For the remaining 5 cases, TLF performs the second best. However, in terms of average performance (as shown in the last row of the table), TLF outperforms existing techniques.

Table 7 presents the classification accuracies of TLF and the existing methods on Reuters-215782 (RT), MNIST+USPS (MU) and COIL datasets. For RT dataset, we present the performances of the techniques of 3 combinations of SDD and TDD in the top 3 rows of the table. Bold values in the table indicate that TLF performs the best in all combinations. For each method, we also calculate the average classification accuracy from the classification accuracies of 3 combinations as shown in the 4-th row of the table. The average classification accuracy of TLF is 0.615. The experimental results clearly indicate that TLF outperforms other methods on RT dataset.

The next 13 rows of Table 7 presents the performances of the techniques of 12 combinations of SDD and TDD that are created from the NG dataset. The best performances are indicated with bold values. The table shows that TLF performs the best in all combinations. We also present the performances of the techniques of 12 combinations of SDD and TDD that are created from the COIL

Table 6: Classification accuracies of TLF and existing methods on OC, NG and VLSC datasets.

Dataset	Domains		Baseline methods				Existing transfer learning methods									TLF
	Source	Target	RF-S	RF-T	SysFor-S	SysFor-T	EasyTL	ARTL	GFK	TCA	JDA	CORAL	BDA	MEDA	SHDA	
OC	amazon	Caltech10	0.153	0.207	0.134	0.229	0.331	0.268	0.233	0.264	0.214	0.249	0.263	0.219	0.277	<b>0.354</b>
	amazon	dslr	0.107	0.087	0.060	0.067	0.048	0.295	0.280	0.309	0.242	0.105	0.242	0.228	0.282	<b>0.313</b>
	amazon	webcam	0.132	0.232	0.104	0.186	0.093	0.286	0.294	0.307	0.296	0.085	0.321	0.279	0.268	<b>0.325</b>
	Caltech10	amazon	0.207	0.254	0.092	0.273	0.248	0.117	0.237	0.165	0.170	0.180	0.175	0.317	0.360	<b>0.367</b>
	Caltech10	dslr	0.107	0.087	0.060	0.067	0.204	0.248	0.269	0.289	0.215	0.204	0.282	0.288	0.295	<b>0.369</b>
	Caltech10	webcam	0.129	0.232	0.071	0.186	0.090	0.246	0.229	0.275	0.221	0.205	0.250	0.229	0.293	<b>0.329</b>
	dslr	amazon	0.197	0.254	0.092	0.273	0.313	0.271	0.223	0.282	0.247	0.323	0.135	0.237	0.193	<b>0.354</b>
	dslr	Caltech10	0.169	0.207	0.102	0.229	0.368	0.288	0.229	0.284	0.240	0.403	0.267	0.238	0.217	<b>0.429</b>
	dslr	webcam	0.196	0.232	0.136	0.186	0.160	0.646	0.466	0.466	0.479	0.180	0.682	0.643	0.336	<b>0.686</b>
	webcam	amazon	0.149	0.254	0.092	0.273	0.328	0.175	0.236	0.112	0.195	0.329	0.232	0.209	0.219	<b>0.358</b>
	webcam	Caltech10	0.153	0.207	0.116	0.229	0.230	0.240	0.219	0.213	0.188	0.234	0.243	0.189	0.218	<b>0.294</b>
	webcam	dslr	0.094	0.087	0.094	0.067	0.186	0.591	0.475	0.490	0.544	0.108	0.557	0.550	0.503	<b>0.627</b>
	Average		0.149	0.195	0.096	0.189	0.216	0.306	0.283	0.288	0.271	0.217	0.304	0.302	0.289	<b>0.400</b>
NG	CSS	CST	0.428	0.478	0.360	0.448	0.528	0.588	0.566	0.561	0.569	0.289	0.579	0.594	0.570	<b>0.616</b>
	CTS	CTT	0.376	0.479	0.374	0.479	0.376	0.480	0.573	0.549	0.553	0.515	0.605	0.549	0.574	<b>0.632</b>
	RSS	RST	0.328	0.478	0.326	0.482	0.413	0.619	0.570	0.530	0.549	0.434	0.547	0.524	0.555	<b>0.627</b>
	RST	RTT	0.325	0.434	0.327	0.382	0.412	0.605	0.573	0.574	0.567	0.526	0.569	0.584	0.538	<b>0.628</b>
	STS	STT	0.422	0.424	0.365	0.380	0.461	0.653	0.517	0.520	0.530	0.424	0.524	0.535	0.565	<b>0.695</b>
	Average		0.376	0.458	0.350	0.434	0.438	0.589	0.560	0.547	0.554	0.438	0.565	0.557	0.560	<b>0.640</b>
VLSC	Caltech101	ImageNet	0.293	0.197	0.294	0.163	0.446	0.651	0.285	0.206	0.316	0.329	0.317	0.543	0.482	<b>0.680</b>
	Caltech101	LabelMe	0.280	0.395	0.280	0.389	0.106	<b>0.601</b>	0.416	0.410	0.389	0.328	0.400	0.531	0.511	0.556
	Caltech101	SUN09	0.294	0.214	0.294	0.183	0.162	0.603	0.372	0.376	0.383	0.329	0.316	0.516	0.500	<b>0.620</b>
	Caltech101	VOC2007	0.346	0.264	0.346	0.266	0.268	0.522	0.470	0.441	0.266	0.346	0.428	0.482	0.476	<b>0.571</b>
	ImageNet	Caltech101	0.317	0.205	0.113	0.243	0.592	0.784	0.589	0.167	0.433	0.411	0.296	0.748	0.761	<b>0.824</b>
	ImageNet	LabelMe	0.078	0.096	0.046	0.061	0.208	0.460	0.130	0.309	0.306	0.205	0.308	0.508	0.526	<b>0.556</b>
	ImageNet	SUN09	0.094	0.127	0.054	0.101	0.210	0.603	0.218	0.304	0.201	0.354	0.316	0.602	0.438	<b>0.620</b>
	ImageNet	VOC2007	0.309	0.305	0.215	0.131	0.371	0.522	0.380	0.132	0.131	0.215	0.128	0.373	0.467	<b>0.571</b>
	LabelMe	Caltech101	0.008	0.236	0.165	0.228	0.149	<b>0.844</b>	0.217	0.404	0.228	0.165	0.731	0.790	0.412	0.838
	LabelMe	ImageNet	0.308	0.208	0.311	0.218	0.195	0.651	0.217	0.169	0.218	0.311	0.170	0.514	0.452	<b>0.680</b>
	LabelMe	SUN09	0.256	0.271	0.267	0.238	0.317	0.603	0.306	0.283	0.383	0.267	0.380	0.530	0.487	<b>0.620</b>
	LabelMe	VOC2007	0.204	0.340	0.240	0.381	0.170	0.522	0.268	0.381	0.381	0.240	0.373	0.490	0.415	<b>0.571</b>
	SUN09	Caltech101	0.024	0.295	0.021	0.283	0.539	<b>0.843</b>	0.300	0.309	0.283	0.302	0.199	0.607	0.452	0.838
	SUN09	ImageNet	0.211	0.215	0.320	0.218	0.174	0.651	0.210	0.195	0.218	0.320	0.517	0.582	0.526	<b>0.680</b>
	SUN09	LabelMe	0.042	0.289	0.102	0.207	0.313	<b>0.601</b>	0.138	0.228	0.368	0.302	0.365	0.517	0.478	0.556
	SUN09	VOC2007	0.047	0.232	0.091	0.228	0.386	0.522	0.300	0.126	0.228	0.091	0.207	0.378	0.321	<b>0.571</b>
	VOC2007	Caltech101	0.228	0.224	0.044	0.247	0.674	0.784	0.645	0.312	0.247	0.044	0.544	0.713	0.542	<b>0.804</b>
	VOC2007	ImageNet	0.711	0.248	0.406	0.289	0.303	0.651	0.431	0.201	0.289	0.406	0.291	0.633	0.417	<b>0.680</b>
	VOC2007	LabelMe	0.193	0.188	0.234	0.215	0.342	<b>0.560</b>	0.277	0.327	0.215	0.234	0.514	0.533	0.453	0.556
	VOC2007	SUN09	0.199	0.150	0.285	0.138	0.334	0.603	0.254	0.310	0.375	0.285	0.161	0.532	0.415	<b>0.620</b>
	Average		0.222	0.235	0.206	0.221	0.313	0.629	0.321	0.280	0.293	0.274	0.348	0.556	0.477	<b>0.651</b>

dataset in the last 13 rows of Table 7. For COIL dataset, TLF outperforms all existing techniques in all combinations.

We present the average classification accuracies (see Table 8) of the TLF and existing techniques on all datasets. Bold values in the tables indicate the best results. From Table 8, we can see that TLF outperforms the other techniques in terms of classification accuracy for all datasets.

#### 5.4. Statistical Analysis of the Results

We now analyze the results by using a statistical non-parametric sign test [29] and Nemenyi [30] test for all datasets in order to evaluate the statistical significance of the superiority of TLF over the existing methods.

We carry out sign test on the results of TLF with other methods (one by one) at the right-tailed

Table 7: Classification accuracies of TLF and existing methods on RT, MU and COIL datasets.

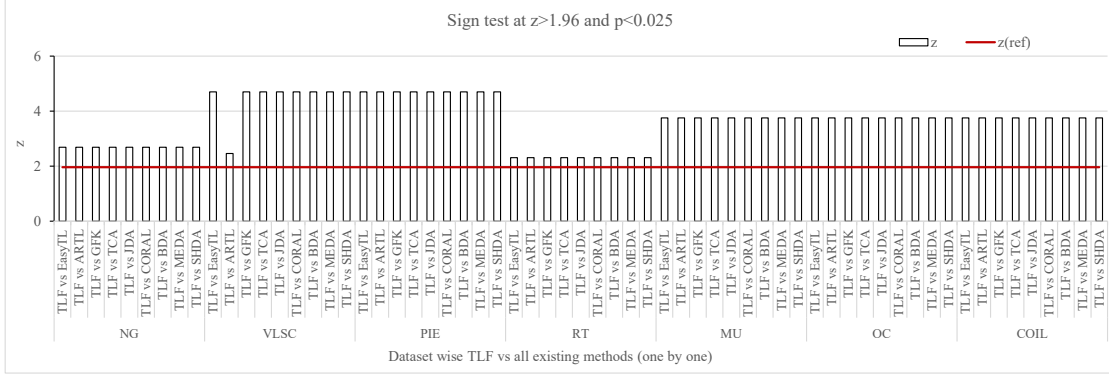
Dataset	Domains		Baseline methods				Existing transfer learning methods									TLF
	Source	Target	RF-S	RF-T	SysFor-S	SysFor-T	EasyTL	ARTL	GFK	TCA	JDA	CORAL	BDA	MEDA	SHDA	
RT	Orgs	People	0.337	0.376	0.320	0.369	0.427	0.552	0.469	0.533	0.539	0.513	0.534	0.513	0.515	<b>0.596</b>
	Orgs	Places	0.322	0.406	0.319	0.395	0.510	0.584	0.464	0.501	0.454	0.510	0.431	0.542	0.527	<b>0.639</b>
	People	Places	0.336	0.372	0.333	0.362	0.412	0.554	0.455	0.470	0.507	0.431	0.467	0.560	0.510	<b>0.610</b>
	Average		0.332	0.385	0.324	0.375	0.450	0.563	0.463	0.501	0.500	0.485	0.477	0.538	0.517	<b>0.615</b>
MU	MUS	MUT	0.100	0.195	0.081	0.081	0.286	0.497	0.313	0.311	0.315	0.321	0.313	0.492	0.312	<b>0.563</b>
	MUS	UMS	0.099	0.195	0.083	0.131	0.290	0.506	0.308	0.312	0.312	0.313	0.326	0.483	0.430	<b>0.551</b>
	MUS	UMT	0.189	0.208	0.175	0.163	0.290	0.485	0.325	0.399	0.397	0.357	0.397	0.462	0.418	<b>0.522</b>
	MUT	MUS	0.084	0.210	0.070	0.192	0.388	0.526	0.417	0.311	0.377	0.418	0.313	0.451	0.317	<b>0.549</b>
	MUT	UMS	0.192	0.196	0.184	0.196	0.370	0.506	0.351	0.383	0.397	0.362	0.399	0.575	0.421	<b>0.615</b>
	MUT	UMT	0.108	0.211	0.069	0.210	0.404	0.447	0.319	0.392	0.314	0.413	0.314	0.410	0.428	<b>0.522</b>
	UMS	MUS	0.108	0.210	0.070	0.192	0.388	0.526	0.317	0.311	0.314	0.410	0.313	0.411	0.417	<b>0.549</b>
	UMS	MUT	0.192	0.207	0.184	0.196	0.420	0.497	0.325	0.380	0.397	0.365	0.395	0.457	0.417	<b>0.631</b>
	UMS	UMT	0.151	0.211	0.069	0.210	0.413	0.447	0.319	0.392	0.414	0.312	0.314	0.410	0.428	<b>0.522</b>
	UMT	MUS	0.188	0.312	0.175	0.293	0.463	0.456	0.353	0.398	0.396	0.365	0.397	0.463	0.423	<b>0.549</b>
	UMT	MUT	0.100	0.195	0.081	0.181	0.386	0.497	0.329	0.411	0.315	0.365	0.413	0.509	0.431	<b>0.631</b>
	UMT	UMS	0.151	0.195	0.083	0.191	0.390	0.506	0.385	0.412	0.412	0.422	0.413	0.514	0.430	<b>0.615</b>
	Average		0.138	0.212	0.111	0.186	0.374	0.491	0.338	0.368	0.363	0.369	0.359	0.470	0.406	<b>0.568</b>
COIL	C1S	C1T	0.164	0.439	0.171	0.369	0.509	0.707	0.627	0.676	0.692	0.496	0.621	0.592	0.566	<b>0.735</b>
	C1S	C2S	0.193	0.476	0.171	0.263	0.503	0.705	0.685	0.708	0.681	0.522	0.575	0.597	0.604	<b>0.733</b>
	C1S	C2T	0.137	0.408	0.128	0.368	0.637	0.728	0.587	0.595	0.654	0.635	0.700	0.670	0.670	<b>0.774</b>
	C1T	C1S	0.124	0.335	0.117	0.336	0.497	0.651	0.685	0.575	0.581	0.486	0.575	0.660	0.616	<b>0.737</b>
	C1T	C2S	0.124	0.476	0.119	0.263	0.642	0.690	0.654	0.597	0.600	0.640	0.600	0.680	0.680	<b>0.775</b>
	C1T	C2T	0.177	0.408	0.164	0.368	0.481	0.637	0.681	0.689	0.579	0.481	0.575	0.650	0.638	<b>0.727</b>
	C2S	C1S	0.124	0.335	0.117	0.336	0.497	0.651	0.585	0.675	0.581	0.486	0.575	0.650	0.616	<b>0.737</b>
	C2S	C1T	0.147	0.439	0.129	0.369	0.645	0.690	0.547	0.596	0.600	0.630	0.685	0.676	0.676	<b>0.772</b>
	C2S	C2T	0.177	0.408	0.164	0.368	0.481	0.637	0.581	0.689	0.579	0.481	0.675	0.680	0.620	<b>0.727</b>
	C2T	C1S	0.107	0.335	0.109	0.336	0.638	0.693	0.654	0.596	0.599	0.622	0.654	0.694	0.693	<b>0.774</b>
	C2T	C1T	0.106	0.439	0.107	0.369	0.509	0.707	0.583	0.576	0.579	0.496	0.582	0.592	0.592	<b>0.735</b>
	C2T	C2S	0.193	0.476	0.171	0.263	0.503	0.705	0.585	0.571	0.581	0.522	0.675	0.599	0.604	<b>0.733</b>
	Average		0.148	0.414	0.139	0.334	0.545	0.683	0.621	0.628	0.609	0.541	0.624	0.645	0.631	<b>0.746</b>

Table 8: Overall classification accuracies of TLF and existing methods on all datasets.

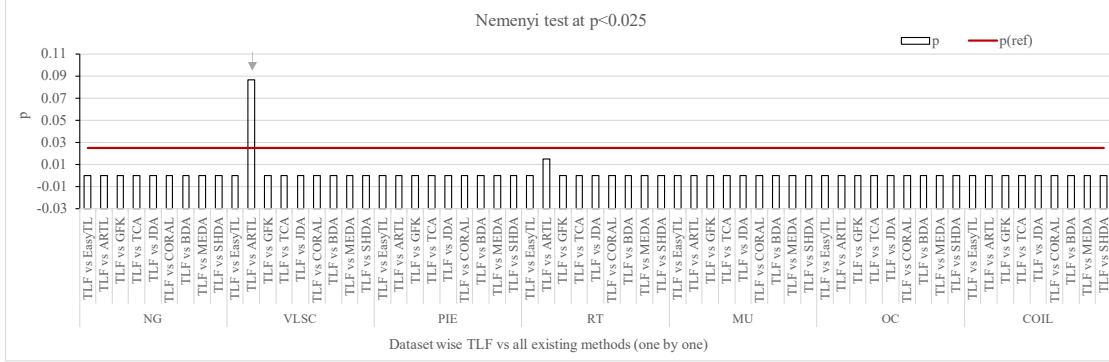
Dataset	Baseline methods				Existing transfer learning methods									TLF
	RF-S	RF-T	SysFor-S	SysFor-T	EasyTL	ARTL	GFK	TCA	JDA	CORAL	BDA	MEDA	SHDA	
PIE	0.086	0.083	0.040	0.063	0.191	0.394	0.379	0.364	0.322	0.200	0.368	0.362	0.278	<b>0.472</b>
OC	0.149	0.195	0.096	0.189	0.216	0.306	0.283	0.288	0.271	0.217	0.304	0.302	0.289	<b>0.400</b>
NG	0.376	0.458	0.350	0.434	0.438	0.589	0.560	0.547	0.554	0.438	0.565	0.557	0.560	<b>0.640</b>
VLSC	0.222	0.235	0.206	0.221	0.313	0.629	0.321	0.280	0.293	0.274	0.348	0.556	0.477	<b>0.651</b>
RT	0.332	0.385	0.324	0.375	0.450	0.563	0.463	0.501	0.500	0.485	0.477	0.538	0.517	<b>0.615</b>
MU	0.138	0.212	0.111	0.186	0.374	0.491	0.338	0.368	0.363	0.369	0.359	0.470	0.406	<b>0.568</b>
COIL	0.148	0.414	0.139	0.334	0.545	0.683	0.621	0.628	0.609	0.541	0.624	0.645	0.631	<b>0.746</b>
Average	0.207	0.283	0.181	0.258	0.361	0.522	0.423	0.425	0.416	0.360	0.435	0.490	0.451	<b>0.585</b>

by considering significance level  $\alpha = 0.025$  (i.e. 97.5% significance level). While we compare TLF with EasyTL (i.e. TLF vs EasyTL) we obtain a z-value (test static value) which is used to determine the significant improvement of TLF over EasyTL. Similarly we obtain z-values for other comparisons based on all datasets as shown in Fig. 8(a). In the figure, each bar represents the z-value of the comparison between TLF and an existing method, whereas the line represents the z-ref value. The z-ref value for  $\alpha = 0.025$  is 1.96. The performance of TLF is significantly better than a method if the z-value of TLF vs the method is greater than the z-ref which is 1.96 in this case for  $\alpha = 0.025$ , as the z-ref value can be obtained from a table [29]. The sign test results (see Fig. 8(a)) indicate that both TLF performs significantly better than the other methods (at  $z > 1.96$ ,  $p < 0.025$ , and right-tailed) on

all datasets.



(a) Statistical Sign test analysis



(b) Statistical Nemenyi test analysis

Figure 8: Statistical significance analysis based on Sign test and Nemenyi test on all datasets.

Similarly, we carry out the Nemenyi test on the results of TLF with other methods (one by one) at the right-tailed by considering significance level  $\alpha = 0.025$  (i.e. 97.5% significance level) as shown in Fig. 8(b). The Nemenyi test results (see Fig. 8(b)) indicate that TLF performs significantly better than the other techniques (at  $p < 0.025$ ) on all datasets except one case marked as down arrow.

### 5.5. Effectiveness Verification of TLF Components

Our proposed TLF framework consists of three main components, namely ridge, MMD and Manifold regularizations. We now evaluate the effectiveness of each component in terms of classification accuracy by carrying out experiments on the PIE and OC datasets. The experimental results are shown in Fig. 9 where the first bar represents the classification accuracy of TLF with all components, the second bar represents the classification accuracy of TLF without ridge regularization, the third represents the classification accuracy of TLF without MMD regularization and the fourth represents the classification accuracy of TLF without manifold regularization. From the figures, we can see the importance

of all components as the classification accuracies of TLF with all components (first bar of the figures) are higher than other settings.

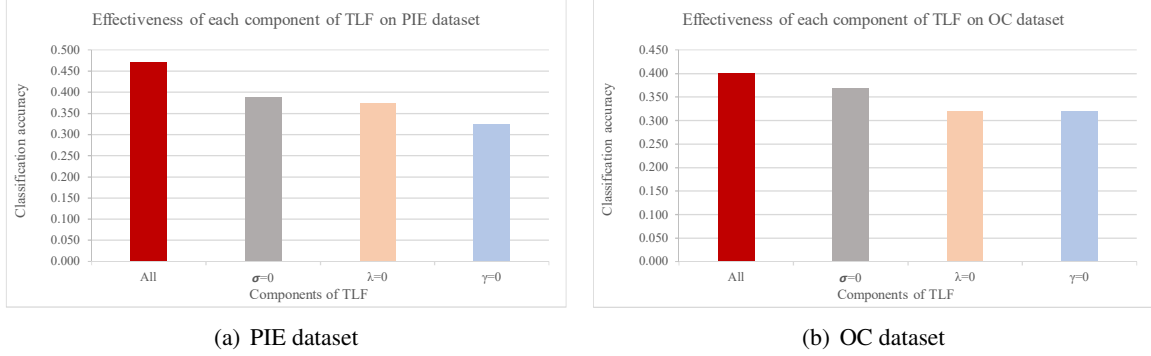


Figure 9: Effectiveness of the use of ridge, MMD and Manifold regularizations in TLF is demonstrated in terms of classification accuracy on PIE and OC datasets.

## 6. Analysis of the Effectiveness of TLF in Some Challenging Situations

After presenting the main experimental results and evaluation in Section 5, we now explore the effectiveness of TLF in some challenging situations, such as when datasets have missing values, as follows.

### 6.1. Handling Datasets with Missing Values

Similar to SHDA [2] and ARTL [3], in TLF we consider the datasets without missing values. However, in some real applications, due to many reasons datasets may contain missing values [31]. In RF [15], missing values are dealt by either (i) using an approach called SRD that simply deletes the records having missing values, or (ii) by imputing missing values with the attribute mean (for numerical) or mode (for categorical) values. If a dataset contains missing values, we suggest to (i) impute the missing values by using a state-of-the-art technique such as SiMI [31], and (ii) consider the imputed dataset as input to TLF.

We examine the effectiveness of TLF in handling missing values on PIE and OC datasets as shown in Fig. 10. For PIE dataset, we artificially create missing values in all source and target datasets. The missing values are created randomly with 5 missing ratios: 10%, 20%, 30%, 40% and 50%, where  $x\%$  missing ratio means  $x\%$  of the total records of a dataset have contained one or more missing values. For example, if a dataset has 100 records then a missing ratio of 50% means that 50 records (out of 100) have at least one missing value. The records are chosen randomly. Once a record is selected,  $y\%$

of total attribute values of the record are randomly made missing. The value of  $y$  is chosen randomly between 1 and 50. For example, if the value of  $y$  is 10 and the dataset has 100 attributes then 10 attribute values of the records are randomly made missing.

For the SRD approach, we first delete the records having missing values from both source and target datasets and then build a classifier for the target domain by applying TLF on the datasets without missing values. The classifier is then used to classify the test data and calculate the classification accuracy. This approach is called “SRD-TLF” in Fig. 10. For an imputation approach, we impute the missing values of both source and target datasets using SiMI [31] and then build a classifier by applying TLF on the datasets without missing values. We then use the classifier to classify the test data and calculate the classification accuracy. This approach is called “SiMI-TLF” in Fig. 10. The average accuracies of all source and target datasets for SRD-TLF and SiMI-TLF on PIE dataset are presented in Fig. 10(a) where the average accuracy of “Original-TLF” is obtained from the TLF column of Table 8. Similarly, for OC dataset, we calculate the average classification accuracies of Original-TLF, SRD-TLF and SiMI-TLF and present them in Fig. 10(b). It is clear from the figures that if a dataset contains missing values, TLF performs better if the missing values are imputed instead of deleting the records having missing values. For small missing ratios, SiMI-TLF achieves almost the accuracy of TLF for a dataset without any missing values.

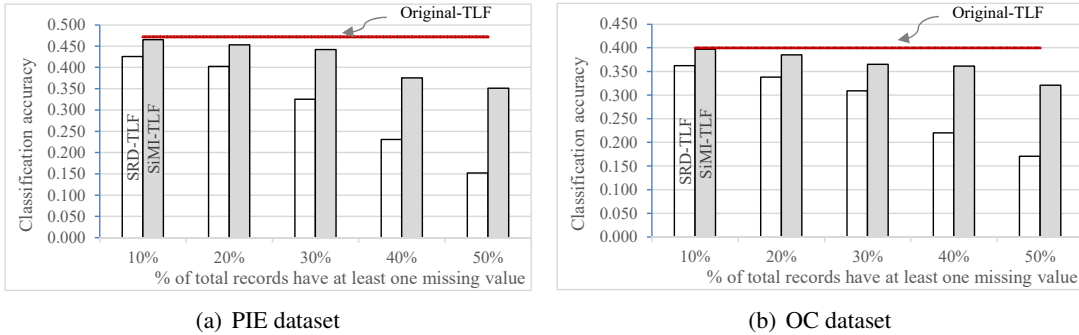


Figure 10: Classification accuracies of Original-TLF, SRD-TLF and SiMI-TLF on PIE and OC datasets.

## 6.2. Handling Class Imbalanced Datasets

Since it is possible to integrate any decision forest algorithm into TLF framework, TLF is capable of handling class imbalanced datasets by integrating an existing algorithm called CSForest [32] which is designated to handle class imbalances problems and we call this variant TLF-C. For implementing the CSForest, we use the Java code from the Weka platform [26]. In our experiment, the

default cost metrics of CSForest are set to: *true-positive*=1, *true-negative*=0, *false-positive*=1, and *false-negative*=5.

We investigate the effectiveness of TLF-C, TLF, CSForest and 3 existing transfer learning methods, namely SHDA, MEDA and ARTL on two class imbalanced datasets, namely segment0 and yeast1 that are publicly available at Keel repository [33]. We create source, target and test datasets from each original dataset as follows. We first create source dataset by randomly selecting 70% records of the original dataset and then create target dataset with the remaining records of the original dataset. After that we divide the target dataset in to test and target datasets by randomly choosing 95% and 5%, respectively, records of the actual target dataset. We repeat this process for 10 runs. For each run, we find the result of a method. We calculate the average result of the 10 runs and present it in Table 9. Since the classification accuracy is not a useful metric for evaluating classifiers built from class imbalanced datasets, we calculate Precision, Recall and F-measure (F1) for each test dataset.

Following the similar process discussed in Section 5.3, we obtain results for the methods, and present in Table 9. Bold values in the table indicate the best results. For the cost metric, TLF-C achieves higher precision, recall and F1 than the other methods. It is clear from table that TLF has the ability to handle class imbalanced datasets by integrating an algorithm such as CSForest [32].

Table 9: Overall Precision, Recall and F1 of TLF and existing methods on two class imbalanced datasets.

Dataset	Precision (higher the better)						Recall (higher the better)						$F_1$ (higher the better)								
	CSForest-S	CSForest-T	SHDA	MEDA	ARTL	TLF	TLF-C	CSForest-S	CSForest-T	SHDA	MEDA	ARTL	TLF	TLF-C	CSForest-S	CSForest-T	SHDA	MEDA	ARTL	TLF	TLF-C
segment0	0.854	0.792	0.715	0.754	0.778	0.812	<b>0.914</b>	0.715	0.701	0.642	0.675	0.688	0.700	<b>0.846</b>	0.778	0.744	0.676	0.712	0.730	0.752	<b>0.879</b>
yeast1	0.541	0.481	0.425	0.445	0.451	0.501	<b>0.654</b>	0.488	0.479	0.408	0.412	0.415	0.452	<b>0.605</b>	0.513	0.480	0.416	0.428	0.432	0.475	<b>0.629</b>

## 7. Conclusion

This paper introduced TLF, a supervised heterogeneous transfer learning framework, which learns a classifier for the target domain having only few labeled training records by transferring knowledge from the source domain having many labeled records. Differing from existing methods, in TLF we simultaneously address two key issues: feature discrepancy and distribution divergence.

To alleviate feature discrepancy, TLF identifies shared label distributions that act as the pivots to bridge the domains (see Step 3 of Algorithm 1 and Fig. 2). To handle distribution divergence, TLF simultaneously optimizes the structural risk functional, joint distributions between domains, and the manifold consistency underlying marginal distributions (see Step 4 of Algorithm 1 and Section 4.1). In TLF, we propose a novel approach to determine nearest neighbors of a record automatically so

that intrinsic properties of manifold consistency can be exploited in detail resulting in a high transfer performance (see Section 4.1 and Fig. 6). Moreover, to avoid negative transfer, we identify transferable records of the source dataset by using the pivots (see Step 3 of Algorithm 1 and Section 4.1).

The effectiveness of TLF is also reflected in the experimental results. We evaluate TLF on seven publicly available natural datasets and compare the performance of TLF against the performance of eleven state-of-the-art techniques including ARTL [3], SHDA [2] and MEDA [4]. From Table 8, we can see that in all datasets TLF outperforms the other techniques in terms of classification accuracy. Statistical sign test and Nemenyi test analyses (see Section 5.4) indicate that TLF performs significantly better than the other methods at  $z > 1.96$ ,  $p < 0.025$  on all datasets.

From the experiments we highlighted the strengths and weaknesses of TLF as follows. The main strengths are: (1) TLF achieves the best classification performance on all datasets over the eleven state-of-the-art techniques (see Table 8), (2) TLF is capable of handling both feature discrepancy and distribution divergence issues simultaneously, (3) TLF has the ability to handle imbalanced datasets (see Section 6.2), and (5) TLF is capable of dealing with datasets having missing values (see Section 6.1). However, like existing methods including ARTL [3], SHDA [2] and MEDA [4], TLF has a limitation on processing multiple source domains. TLF is now suitable for handling only a single source domain at a time.

In future, we plan to explore the effectiveness of combining records from multiple source domains to learn classifiers for the target domain.

## References

- [1] S. Niu, Y. Liu, J. Wang, H. Song, A decade survey of transfer learning (2010–2020), *IEEE Transactions on Artificial Intelligence* 1 (2) (2020) 151–166.
- [2] S. Sukhija, N. C. Krishnan, Supervised heterogeneous feature transfer via random forests, *Artificial Intelligence* 268 (2019) 30–53.
- [3] M. Long, J. Wang, G. Ding, S. J. Pan, S. Y. Philip, Adaptation regularization: A general framework for transfer learning, *IEEE Transactions on Knowledge and Data Engineering* 26 (5) (2014) 1076–1089.
- [4] J. Wang, Y. Chen, W. Feng, H. Yu, M. Huang, Q. Yang, Transfer learning with dynamic distribution adaptation, *ACM Transactions on Intelligent Systems and Technology (TIST)* 11 (1) (2020) 1–25.
- [5] L. Bruzzone, M. Marconcini, Domain adaptation problems: A dasvm classification technique and a circular validation strategy, *IEEE transactions on pattern analysis and machine intelligence* 32 (5) (2009) 770–787.



- [6] J. Wang, Y. Chen, H. Yu, M. Huang, Q. Yang, Easy transfer learning by exploiting intra-domain structures, in: IEEE International Conference on Multimedia & Expo (ICME), 2019.
- [7] S. J. Pan, Q. Yang, A survey on transfer learning, IEEE Transactions on knowledge and data engineering 22 (10) (2010) 1345–1359.
- [8] S. J. Pan, J. T. Kwok, Q. Yang, et al., Transfer learning via dimensionality reduction., in: AAAI, Vol. 8, 2008, pp. 677–682.
- [9] M. Belkin, P. Niyogi, V. Sindhwani, Manifold regularization: A geometric framework for learning from labeled and unlabeled examples., Journal of machine learning research 7 (11).
- [10] W. Li, L. Duan, D. Xu, I. W. Tsang, Learning with augmented features for supervised and semi-supervised heterogeneous domain adaptation, IEEE transactions on pattern analysis and machine intelligence 36 (6) (2013) 1134–1148.
- [11] J. T. Zhou, I. W. Tsang, S. J. Pan, M. Tan, Heterogeneous domain adaptation for multiple classes, in: Artificial intelligence and statistics, 2014, pp. 1095–1103.
- [12] W. Dai, Q. Yang, G.-R. Xue, Y. Yu, Self-taught clustering, in: Proceedings of the 25th international conference on Machine learning, 2008, pp. 200–207.
- [13] Y. Lu, W. Wang, C. Yuan, X. Li, Z. Lai, Manifold transfer learning via discriminant regression analysis, IEEE Transactions on Multimedia.
- [14] V. Vapnik, Statistical Learning Theory, John Wiley, New York, 1998.
- [15] L. Breiman, Random forests, Machine learning 45 (1) (2001) 5–32.
- [16] J. Wang, Y. Chen, S. Hao, W. Feng, Z. Shen, Balanced distribution adaptation for transfer learning, in: The IEEE International conference on data mining (ICDM), 2017, pp. 1129–1134.
- [17] B. Saha, S. Gupta, D. Phung, S. Venkatesh, Multiple task transfer learning with small sample sizes, Knowledge and information systems 46 (2) (2016) 315–342.
- [18] E. Zhong, Transfer learning resources, <https://www.cse.ust.hk/TL/>, accessed April 25, 2021 (2020).
- [19] S. Ben-David, J. Blitzer, K. Crammer, F. Pereira, Analysis of representations for domain adaptation, Advances in neural information processing systems 19 (2006) 137–144.
- [20] J. Wang, et al., Everything about transfer learning and domain adaption, <http://transferlearning.xyz>, accessed May 29, 2021 (2020).
- [21] J. Wang, W. Feng, Y. Chen, H. Yu, M. Huang, P. S. Yu, Visual domain adaptation with manifold embedded distribution alignment, in: Proceedings of the 26th ACM international conference on Multimedia, 2018, pp. 402–410.
- [22] S. J. Pan, I. W. Tsang, J. T. Kwok, Q. Yang, Domain adaptation via transfer component analysis, IEEE Transactions on Neural Networks 22 (2) (2011) 199–210.
- [23] B. Sun, J. Feng, K. Saenko, Return of frustratingly easy domain adaptation, AAAI 6 (7).

- [24] M. Long, J. Wang, G. Ding, J. Sun, P. S. Yu, Transfer feature learning with joint distribution adaptation, in: Proceedings of the IEEE international conference on computer vision, 2013, pp. 2200–2207.
- [25] M. Z. Islam, H. Giggins, Knowledge discovery through sysfor: a systematically developed forest of multiple decision trees, in: Proceedings of the Ninth Australasian Data Mining Conference-Volume 121, Australian Computer Society, Inc., 2011, pp. 195–204.
- [26] E. Frank, M. A. Hall, I. H. Witten, The weka workbench. online appendix for "data mining: Practical machine learning tools and techniques" (2016).
- [27] N. Jamali, C. Sammut, Majority voting: Material classification by tactile sensing using surface texture, IEEE Transactions on Robotics 27 (3) (2011) 508–521.
- [28] A. Bifet, G. Holmes, R. Kirkby, B. Pfahringer, MOA: massive online analysis, J. Mach. Learn. Res. 11 (2010) 1601–1604.
- [29] R. D. Mason, D. A. Lind, W. G. Marchal, Statistics: an introduction, Duxbury Press, 1994.
- [30] J. Demšar, Statistical comparisons of classifiers over multiple data sets, Journal of Machine learning research 7 (Jan) (2006) 1–30.
- [31] M. G. Rahman, M. Z. Islam, Missing value imputation using decision trees and decision forests by splitting and merging records: Two novel techniques, Knowledge-Based Systems 53 (2013) 51 – 65.
- [32] M. J. Siers, M. Z. Islam, Novel algorithms for cost-sensitive classification and knowledge discovery in class imbalanced datasets with an application to nasa software defects, Information Sciences 459 (2018) 53–70.
- [33] J. Alcalá-Fdez, A. Fernández, J. Luengo, J. Derrac, S. García, L. Sánchez, F. Herrera, Keel data-mining software tool: data set repository, integration of algorithms and experimental analysis framework., Journal of Multiple-Valued Logic & Soft Computing 17.